Title

A comprehensive review of synthesis, structure, properties, and functionalization of MoS2; emphasis on drug delivery, photothermal therapy, and tissue engineering applications

Authors

Pourmadadi, Mehrab
Tajiki, Alireza
Hosseini, Seyede Mahtab
et al.

Publication Date

2022-10-01

DOI

10.1016/j.jddst.2022.103767

Journal of Drug Delivery Science and Technology 76 (2022) 103767

Contents lists available at ScienceDirect

Journal of Drug Delivery Science and Technology

journal homepage: www.elsevier.com/locate/jddst

Review article

A comprehensive review of synthesis, structure, properties, and functionalization of MoS_2; emphasis on drug delivery, photothermal therapy, and tissue engineering applications

Mehrab Pourmadadi [a], Alireza Tajiki [b], Seyede Mahtab Hosseini [b], Amirmasoud Samadi [a,c], Majid Abdouss [b,*], Shirin Daneshnia [b], Fatemeh Yazdian [d]

[a] Department of Biotechnology, School of Chemical Engineering, College of Engineering, University of Tehran, Tehran, Iran
[b] Chemistry Department, Amirkabir University of Technology, Tehran, 1591634311, Iran
[c] Department of Chemical and Biomolecular Engineering, University of California, Irvine, CA, USA
[d] Department of Life Science Engineering, University of Tehran, Tehran, Iran

ARTICLE INFO

Keywords:
Molybdenum disulfide (MoS_2)
Drug delivery
Photothermal therapy
Tissue engineering
Synthesis
Properties

ABSTRACT

This review article is focused on the drug delivery platforms and cancer treatment systems recently developed based on molybdenum disulfide (MoS_2) nanosheets. Two-dimensional MoS_2 can be used as a therapeutic nanoparticle and tissue engineering scaffold for tumor healing. Structure, different synthesis methods, unique properties, and surface modification approaches of MoS_2 as a newly emerging carrier for a wide range of drugs were comprehensively discussed. Numerous examples of drug delivery systems based on these carriers were introduced, and their key characteristics and highlights were compared in tables. Striking features in the two-dimensional nanostructure state like the high degree of anisotropy, mechanical strength, biocompatibility, large surface area, availability of surface modification methods for enhanced functionality, distinctive band gap structure, high absorbance in the near-infrared region, and remarkable magnetic attributes render MoS_2 an ideal and attractive candidate to develop multifunctional platforms for combined chemotherapy and photothermal therapy as well as biosensing and bioimaging applications. These properties have piqued the interest of many researchers and led them to study the versatile biomedical applications of these materials, particularly drug delivery and photothermal therapy. Finally, the opportunities, remaining challenges, and future prospects ahead in this area were mapped out.

1. Introduction

The drug administration is via oral and non-oral routes. Oral drug administration involves the gastrointestinal tract, and the drug release starts in the stomach and is absorbed in the intestine. In contrast, non-oral drug delivery primary routes include inhalation, transdermal, and ophthalmic. The conventional oral drug delivery dosage forms are pills, capsules, and syrups, while the non-oral drug delivery is accomplished via injections, eye drops, and topical creams [1]. Maintaining the drug concentration above the minimum effective concentration (MEC), control over the release profile, and precision dosing are the primary concerns regarding conventional delivery methods due to the lack of targeted delivery. A lack of control over the release profile impedes conventional drug delivery methods since controlling the release profile and using a proper concentration are crucial to address side effects on healthy organs and meet the patient's treatment needs until the next dose administration with minimum fluctuations in drug concentration in the patient's body [2,3].

Targeted drug delivery systems are a promising solution to control the delivery of drugs to a specific site with a precise dose for a predetermined duration to provide effective drug concentrations at the target site, reduce drug degradation, and restrict drug distribution to other healthy tissues to minimize side effects, and increase the therapeutic effects subsequently [4]. Today, various nanostructures are used as drug carriers in modern drug delivery platforms. Nanostructures have been in the spotlight among fabricated delivery systems due to their unique properties, such as loading and releasing the drug under certain conditions [5–7]. Each drug nanocarrier system has its chemical,

* Corresponding author.
E-mail address: phdabdouss44@aut.ac.ir (M. Abdouss).

https://doi.org/10.1016/j.jddst.2022.103767
Received 22 May 2022; Received in revised form 19 August 2022; Accepted 29 August 2022
Available online 3 September 2022

physical, and morphological properties. Different chemical interactions, such as covalent, hydrogen, or physical interactions such as electrostatic and Van der Waals, determine binding tendencies to various polar and non-polar drugs [8]. In addition, other factors such as different morphologies of nanosystems play a vital role in the controlled drug release profile. So far, several examples of targeted drug delivery systems using a variety of nanostructures such as carbon-based nanomaterials [9] (graphene [10], graphene oxide [11,12], single and multi-wall carbon nanotubes [13,14], fullerenes [15] and others), graphitic carbon nitrides [16], transition metal dichalcogenides [17], hexagonal boron nitrides [18], metal and metal oxide nanoparticles [19–21], halloysite nanotubes [22], quantum dots [23], etc. have been introduced.

Photothermal therapy (PTT) is laser irradiation of target tissue with the help of light-absorbing materials. This causes hyperthermia, which is used to treat cancer and effectively prevent bacterial infections [20]. Combining photothermal therapy and drug delivery systems increases the chances of treating various cancers. Photothermal materials are usually nanostructures that kill cancer cells by absorbing light in specific wavelength ranges and converting it to heat in a particular body area [24]. Noble metal and metal oxide nano particles [25], transition metal sulfides [26], carbon-based nanomaterials [27], quantum dots [28], organic dyes [29], polymeric nano particles [30], etc. are widely used as a photothermal agent in PTT.

Recently, molybdenum disulfide (MoS_2) nanosheets have been frequently used as nanocarriers in targeted drug delivery systems, photothermal therapy, and tissue engineering due to their extraordinary properties, which will be discussed in the following sections [31]. Furthermore, to improve the physical and chemical properties of MoS_2 nanosheets, their surface has been modified by various methods. This review article deals with the different drug delivery platforms, photothermal therapy, and tissue engineering systems based on MoS_2 and its derivatives and their preparation approaches.

2. Structure and properties of MoS_2

Two-dimensional transition metal dichalcogenides (TMDCs) are graphene-like compounds that have attracted much research interest. Molybdenum disulfide (MoS_2) is one of the most common types of TMDCs [32]. MoS_2 is naturally found in a triangular prismatic structure in which the structure is AbA BaB, whereas MoS_2 is synthesized in the form of a side rhombus with the structure of AbA CaC BcB [33]. MoS_2 is unstable in the octagonal phase and turns into a triangular prism phase by raising the temperature to 300 °C. For this purpose, 2H–MoS_2 is synthesized [34]. In MoS_2, quaternary molybdenum cations are connected to six sulfur anions, forming a charter. As shown in Fig. 1 (a), in the structure of a triangular prism of molybdenum disulfide, the distance of sulfurs in the network is a = 3.16 A°. Also, the distance between two sulfurs in two consecutive units is equal to c = 12.3 A° [35]. Due to the diversity of the order of X-M-X stacks in dichalcogenide transition metals, three different types of crystal structures, including the hexagonal 2H phase (AbA BaB stacking sequence), the octahedral 1T phase (AbC AbC stacking sequence), and the rhombohedral 3R phase (AbA CaC BcB stacking sequence) have been considered for this material. Uppercase and lowercase letters show the S and Mo layers, respectively [36]. In a molybdenum disulfide monolayer, (+4) Mo and S (-2) are ordered in a sandwich structure with covalent bonds in an S–Mo–S sequence. On the other hand, the sandwich layer interacts with the rather weak Van der Waals forces. Usually, each layer has a thickness of 0.65 nm. This unique structure makes it easy to be exfoliated due to the weak interlayer interactions [37,38]. MoS_2 in bulk form consists of layers with an outline in the style of one Mo atom surrounded by six sulfur atoms. MoS_2 consists of layers that are three atoms thick. In MoS_2 configuration, adjacent layers are related to weak Van der Waals forces, which facilitate the layers of MoS_2 sliding on one another [39].

Two-dimensional materials exhibit new mechanical, thermal, and optoelectrical properties that are quite different from their bulk state [40]. Molybdenum disulfide is a two-dimensional material with extraordinary properties in the two-dimensional structure like distinctive band gap structure, high mobility, high absorbance in the near-infrared region, remarkable magnetic features, mechanical strength, and high surface area to volume ratio, which can be used in nanostructured and photonic devices [41]. This article briefly describes the properties of this material.

2.1. Electronic and optical properties

Graphene has attracted significant consideration in recent years due to its unique structure and remarkable electronic properties; yet, it's a

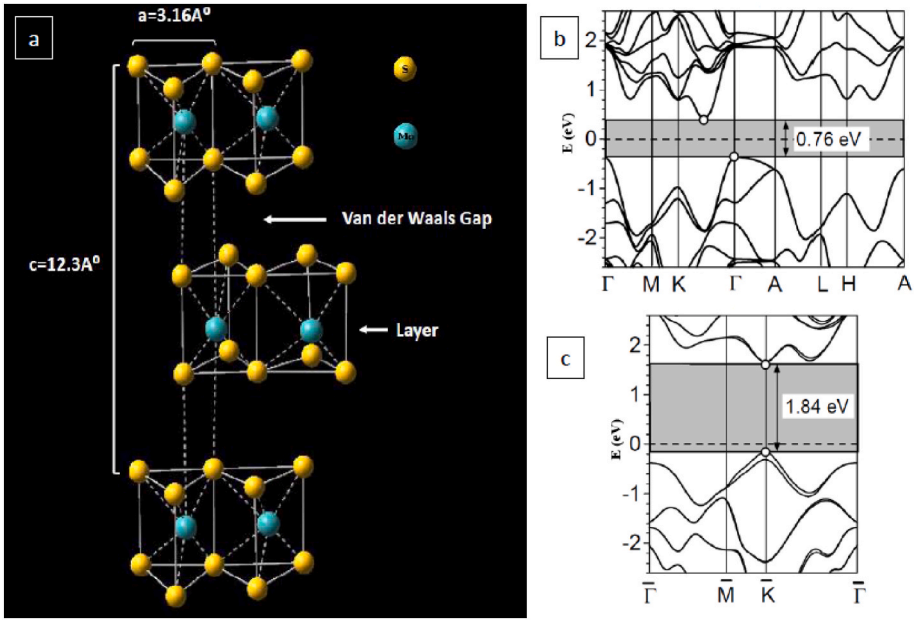

Fig. 1. (a) Three layers of MoS_2 structure. In figures (b) and (c), the band structures of bulk MoS_2 and MoS_2 monolayers are shown, respectively. Shaded areas denote circles that mark the band gaps, valence band maxima, and conduction band minima [48].

zero-band semi-metal that makes the switching ratio of optical electronic devices with low and weak performance on logical devices [42]. Two-dimensional nanomaterial semiconductors have many potential applications due to their large surface areas and unique electronic properties [43]. The discovery of a direct energy gap of approximately 1.9 eV in a molybdenum disulfide monolayer (suitable as a switching nanodevice) and the semiconductor properties of two or more layers promise various applications in electronic devices [39,44]. In recent years, devices based on multilayer molybdenum disulfide, such as transistors, sensors, optical detectors, etc., have been introduced [45]. In dichalcogenide transition metals of group six of the periodic table, the energy gap size in the monolayer increases by 50% compared to the bulk mode [46]. Bulk MoS_2 is an indirect gap semiconductor with a band gap of about 1 eV, with a valence band utmost at point Γ and a conduction band minimum (CBM) at the midpoint along the lines of symmetry ΓK. In contrast, monolayers of the same material have a direct gap between the edge of the conduction band and the valence at point K (Fig. 1 (b), (c)) [47,48]. Due to quantum effects, the transition from an indirect gap in bulk mode to a direct gap in monolayer mode results in enhanced photoluminescent features of single-layer films [49,50], as evidenced by the change in the energy gap from 1.2 eV in bulk molybdenum disulfide to a direct gap in the monolayer with a value of approximately 1.9 eV [44]. This feature allows for numerous optical and electronic applications. Besides, MoS_2 is a non-magnetic material in the bulk state, but in the nanostructured state, the edge atoms of the sheets exhibit different magnetic properties appropriate for developing nanodevices [51].

2.2. Friction properties

Researchers have determined that mechanical friction accounts for about 30% of the total energy produced yearly in the world. Addressing friction challenges like wear, tear, and ultimately the failure of mechanical systems can lower maintenance expenditure and create a more prosperous economy [52]. Two-dimensional nanomaterials with a few atomic layers thickness and crystalline structures, such as graphene and MoS_2, are broadly utilized as solid-state lubricants due to their superior tribological and anti-abrasion properties [53]. MoS_2 is a well-known layered solid lubricant that has been used as a lubricant for several centuries [54]. More recently, MoS_2 in various shapes, such as nanoparticles [55], nanotubes [56], and platelets [57], started to be utilized as additives in lubricant oils as well. The role of MoS_2 as a lubricant is due to its frictional properties, ascribed to its physical and chemical properties. Low-friction and easy-to-separate molybdenum disulfide for the material and its inherent crystalline structure are unique features of MoS_2 [54]. For thick layers, a material must meet three basic conditions to achieve low friction: 1- a transfer film must be made on its counterpart so that MoS_2 can slide against itself; 2- MoS_2 grains at the joint surface must either redirect or recently form with base plates (0001) parallel to the slip direction; 3- contaminants should be minimized [58].

2.3. Mechanical properties

As mentioned before, having a two-dimensional shape, being part of the transition metal dichalcogenide family, and having high strength characteristics are among the aspects that render MoS_2 an attractive compound in the industry [59]. In structural applications, one of the most attractive properties of MoS_2 is the elastic firmness within the sheet of full sp^3 covalent bond structures [60]. A single-layer MoS_2 sheet has threefold atomic plates with various atomic accumulating subsequence, in which a close pack of molybdenum (Mo) is surrounded by two packed sulfur atomic layers (S) with three layers as appears in Fig. 1 (a) [59,61].

3. Synthesis of MoS_2

Many approaches have been established to develop and fabricate nanostructures with regulated size, shape, dimensions, and structure in zero-dimensional, one-dimensional, two-dimensional, and three-dimensional. These methods are a collection of physical and chemical procedures that can be divided into two groups: top-down and bottom-up [62]. These methods have a crucial role in modern industry and are also effective in nanotechnology. The methods of these two categories will be explained in the following sections.

The top-down method reduces the dimensions of bulk material to the desired dimensions and involves crushing or splitting materials in size into nanoscale structures or particles. This approach includes lithium intercalation, mechanical exfoliation, liquid-phase exfoliation, etc. [63]. On the other hand, the bottom-up approach implies that growth starts from atoms and molecules and produces larger structures. The construction of materials from the base, i.e., atom to atom, molecule to molecule, or cluster to cluster, is attributed to the gas or solution phase. The desired structure can be achieved by manipulating the arrangement of atoms and molecules; thus, this method allows it to manipulate properties such as size, shape, stoichiometry, cross-section, porosity, and surface arrangement. Chemical vapor deposition (CVD), hydrothermal, chemical synthesis, and other methods are used in this technique [64].

3.1. Mechanical exfoliation

This method was first used by Noselof et al. [65]. The group isolated graphene using mechanical methods and examined it using atomic force and tunnel scanning microscopes. Similar to the technique used for graphene, molybdenum disulfide nanosheets can be created. This involves pouring some of molybdenum disulfide onto the adhesive and gluing the two sides of the adhesive together. This method is repeated many times to achieve nanometer-thick layers. After the layers are ready, they are transferred to a clean silicon oxide substrate containing MoS_2 (Fig. 2 (a)) [66,67]. Mechanical exfoliation is limited due to the lack of scalability. This method is a low-cost method, but the efficiency is very low in this method. Therefore, it is not feasible for industrial purposes [68].

3.2. Liquide phase exfoliation

Liquid Phase Exfoliation (LPE) is a simple and inexpensive technology that enables high-quality mass production. The LPE promotes the formation of thin layers and connections. It is flexible, and the simplest effect of exfoliation is to significantly increase the available surface area of material and make it stable to produce two-dimensional nanosheets [69,70]. LPE in ultrasonic baths (with solvent and suitable mechanical force) has attracted consideration to produce MoS_2 nanosheets with a high level of productivity. The layer is separated from the bulk material by long-term sonication. The layer thickness of MoS_2 nanosheets is determined by the solvent type and the dissolved concentration [71]. In this method, a certain amount of molybdenum sulfide powder is first added to 1-dodecyl-2-pyrrolidinone (N12P) in a ratio of 10 mg/ml. The mixture is placed in an ultrasonic bath for 1 h continuously using an ice water bath to maintain a stable temperature. Eventually, the resulting solution is centrifuged at 1500 rpm for 45 min, and the molybdenum sheets are separated [72]. The most common solvent used to exfoliate MoS_2 nanosheets is N-methyl-2pyrrolidine (NMP), which has the disadvantage of a slow volatility rate. In a study by May Sahoo et al., they used a cost-effective method for synthesizing multilayer MoS_2 nano-sheets using acetone as a solvent by varying the concentrations with long ultrasound times (without adding any surfactant). Different concentrations (0.08–0.4 mg/ml) were prepared from the MoS_2 sample in acetone solvent, and then the mixture was placed in an ultrasonic bath for 30 h and then centrifuged at 1328 RCF for 2 h (Fig. 2 (b)) [71].

3.3. Lithium intercalation

The intercalation of small alkali metal salts has developed as a

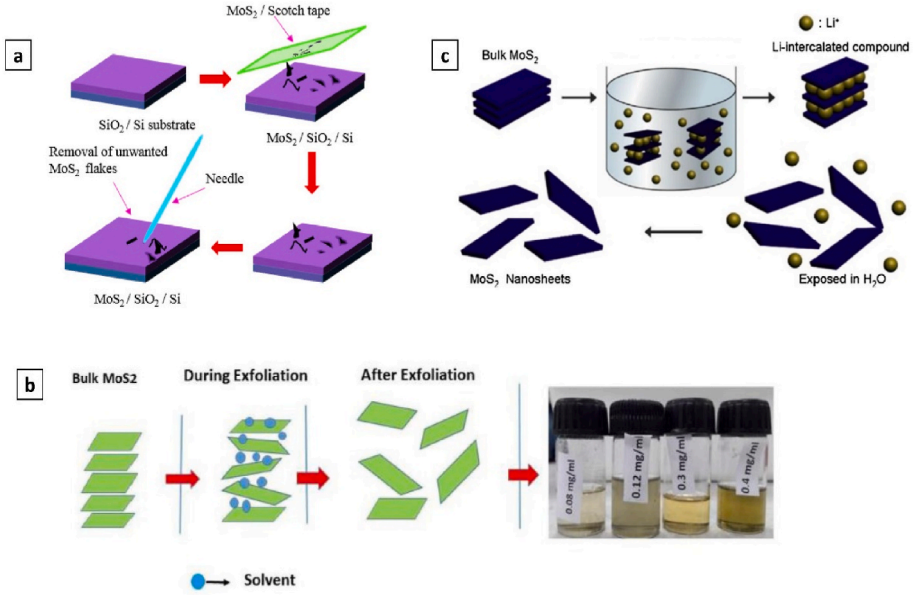

Fig. 2. (a) Schematic of mechanical exfoliation process of MoS_2 flakes [66]; (b) Schematic illustration of liquid phase exfoliation synthesis process of MoS_2 nanosheets [71]; (c) The lithium intercalation and exfoliation process of MoS_2 nanosheets is depicted schematically [74].

promising way to exfoliate transition-metal dichalcogenide (TMDC) nanosheets. Studies have shown that small lithium metal ions are by far the foremost efficient intercalants in bulk transition-metal dichalcogenides. In nearly all changes in the method of intercalation and exfoliation of lithium, the reaction of lithium ions mixed with water (via ultrasound) to make LiOH and H_2 is the driving force for exfoliation. The growth and distension of hydrogen gas between the layered crystals create an internal exfoliation force that allows the transition-metal dichalcogenide (TMDC) nanosheets to separate [73]. The most common synthesis method is inserting Li ions between molybdenum disulfide plates. In this process, n−butyllithium is mixed with molybdenum disulfide powder and placed in a flask filled with argon gas for two days. Then, it is filtered when $LixMoS_2$ is made and washed with hexane to remove excess lithium and organic residues. After the entry of lithium ions, the mixture is laminated under ultrasound waves, and then the excess lithium is separated in the form of LiOH by centrifugation (Fig. 2 (c)) [34,74]. The efficiency of this method is so high that nearly 100% of the products are atomic in size. The main advantage of the lithium intercalation method is the access to the metal phase 1T, which is created by transferring the load from Li to MoS_2. The 2H to 1T atomic structure rearrangements in this method occur [75].

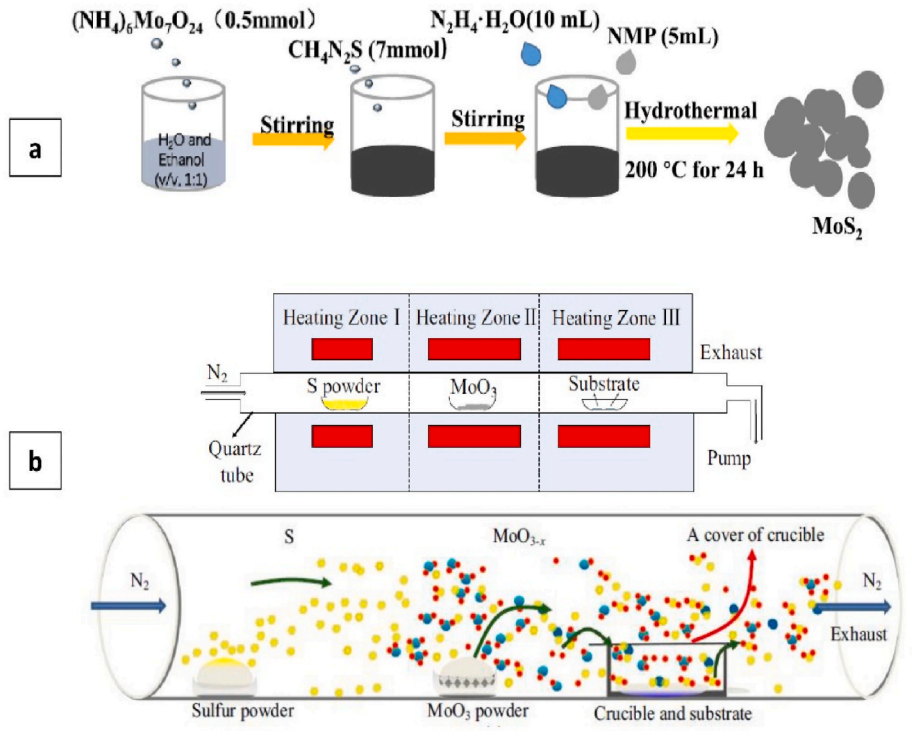

Fig. 3. (a) Schematic diagram of MoS_2 synthesis with hydrothermal method [77]; (b) Schematic view of chemical vapor deposition method [82].

3.4. Hydrothermal synthesis

The hydrothermal approach is mainly utilized for the synthesis of MoS_2 nanostructures. Due to fabrication at low temperature, this approach has the cap potential to manipulate the morphology, provides uniformity and high crystallinity, has acceptable performance, and is also a cost-effective method that can be widely used [76].

In this method, thiourea and $(NH_4)_6Mo_7O_{24} \cdot 4H_2O$ in a certain mass ratio are added to a solution of a mixture of deionized water and ethanol in a specific ratio subject to stirring. Then a certain amount of N-methyl-2- pyrrolidone and $N_2H_4{\cdot}H_2O$ is added to the solution and stirred to obtain a uniform mixture. Then, it is transmitted into an autoclave and set at 200 °C for 24 h. After cooling, the powder was collected using a centrifuge, washed with water and ethanol, and placed in an

Table 1
Summary of synthesis techniques.

Technique	Description	Features	Year	Reference
Lithium intercalation	Researchers have discovered since 1983 that $LixMoS_2$ undergoes a phase transition when $0.2 < x < 1$. Lithium intercalation can be conducted with chemical and electrochemical approaches.	Facilitates manipulation of photoluminescent properties High yield of monolayer MoS_2 Time-consuming Producing highly pyrophoric organolithium compounds that should be handled away from oxygen and moisture	2002	[83–86]
Chemical Vapor Deposition (CVD)	MoO_3 and sulfur are commonly used in the chemical vapor deposition method MoO_3 and S are first evaporated at a specific temperature in the chemical vapor deposition technique. The S vapor then passes MoO_3 through an inert gas such as argon. MoS_2 layers are then synthesized at 850 °C for 20 min and formed on a SiO_2 substrate.	Suitable for producing high-purity single-layer transition metal oxide films	2003	[80,87]
Mechanical exfoliation	Pouring some of molybdenum disulfide onto the adhesive and repeatedly gluing the two sides of the adhesive together to produce nanometer-thick layers. Then, transferring layers to a clean silicon oxide substrate containing MoS_2.	Flakes are not controlled in thickness, shape, size, or position Demonstrates field-effect mobility values significantly higher than the CVD method Low-cost method Very low efficiency Not viable for industrial applications Requiring high temperature	2005	[65,88]
Hydrothermal	MoS_2 was prepared by using $(NH_4)_6Mo_7O_{24}{\cdot}4H_2O$, sulfocarbamide $(CS(NH_2)_2)$, and oxalic acid $(H_2C_2O_4{\cdot}2H_2O)$ as precursors. Powders of these compounds were mixed with water and kept at 200 °C for 24 h. Then, the gray solid was calcined in a furnace at 500 °C for 2 h with argon gas flow.	Low yield Forming microparticles Lengthy process Dependent on the solubility of chosen precursors High temperature and pressure Easier to form nanocomposites with other materials such as carbon nanotubes and graphene Fabrication at low temperature Having cap potential to manipulate the morphology Providing uniformity and high crystallinity, Cost-effective	2009	[88,89]
Liquid exfoliation	A certain amount of molybdenum sulfide powder is first added to 1-dodecyl-2-pyrrolidinone (N12P) in a 10 mg/ml ratio. The mixture is placed in an ultrasonic bath for 1 h continuously using an ice water bath to maintain a stable temperature. Ultimately, the solution is centrifuged at 1500 rpm for 45 min to separate MoS_2 nanosheets.	Simple and inexpensive Enabling high-quality mass production Promoting the formation of thin layers A flexible method Significant increase in the available surface area Stable production of two-dimensional nanosheets Use of toxic solvents Possibility of producing micro sheets	2011	[72,88,90]
Solvothermal method	Two-dimensional MoS_2 nanosheets were efficiently produced using a solvothermal technique with the help of oleylamine in this paper. Oleylamine triggered the development of a single or few layers of 2D MoS_2.	Producing large amounts of two-dimensional MoS_2 nanosheets Low cost Simple operation Less adverse environmental impacts	2018	[91]
Probe-Tip sonication	This study used a simple, eco-friendly, green, and cost-effective approach to synthesize water-soluble MoS_2 nanosheets. The consecutive batch/synthesis method significantly improved the efficiency (up to 100%) of MoS_2 nanosheets.	Producing water-soluble nanosheets High yield Operated in batch manner	2020	[88]
Microwave synthesis	MoS_2 nanosheets are produced using microwave synthesis in a concise time of 30 min.	The significant disadvantage is using toxic solvents Very easy to operate Consuming less energy Short process	2020	[88,92]
Ball milling and chemical intercalation	An innovative approach to fabricate MoS_2 nanofilms using a hydrazine-assisted ball mill through the synthesizing effect of chemicals and mechanical peeling, nanoflakes with a lateral dimension of 600–800 nm and a thickness of less than 3 nm, as well as high crystallinity in the 2H semiconducting phase.	Low yield Use of toxic solvents Producing disordered nanosheets	2020	[88,93]
Sulfidation	In this study, by reducing the deposited amorphous MoO_3-x layer thickness to 1 nm, a predominantly monolayer MoS_2 film is obtained after sulfidation at 780 °C.	Reducing the effect of gas flows occurring in CVD Producing self-aligned patterns of MoS_2 Easy control over Mo amounts	2021	[94]
Magnetron sputtering	MoS_2 films were grown on a silicon bed by radio frequency (RF) sputtering and tested at different temperatures. It was concluded that by increasing the deposition temperature from 150 °C to 300 °C, crystal quality, optical bandgap, resistance, and thickness were increased.	Vulcanization results in polycrystalline blocks, making it hard to fabricate single-layer film Significant advantages include high deposition rates, ease of sputtering various metals, ability to produce films with high purity, perfect uniformity	2021	[95,96]

exceedingly vacuum oven that was dried at 60 °C for 6 h (Fig. 3 (a)) [77]. In another study, a specific amount of sodium molybdate and thiourea was dissolved in a certain quantity of deionized water at different concentrations with a specific mass ratio. Then, the product was stirred for half an hour. Next, a particular amount of acid was added to accelerate the formation of the MoS_2 phase. The mixture was then transferred to an autoclave and placed at 200 °C for 24 h. The mixture was centrifuged and washed several times with deionized water and ethanol. In the end, it was dried at 80 °C for 12 h. In the hydrothermal process, the regulation of the pH, the sulfur source's content, and the precursor's concentration are critical experimental conditions to control the thickness of the nanosheets. The pH setting affects the sulfurated or reduction reaction during the synthesis of MoS_2, so the thickness declines as the pH rises [78].

3.5. Chemical Vapor Deposition (CVD)

Chemical vapor deposition is a bottom-up method and a vital synthesis method for two-dimensional materials and is also preferred for defect management, crystallinity, and morphology [79]. CVD has recently become an essential method for producing high-purity single-layer transition metal oxide films. CVD involves the chemical reaction of vapors on the substrate to produce large-scale thin films [80]. MoO_3 and sulfur are commonly used in the chemical vapor deposition technique, and the substrate is typically made of SiO_2. The substrate is cleaned with ethanol, acetone, and deionized water before use. MoO_3 powder is generally placed in an Alumina Combustion Boat near the center of the furnace heating zone, while sulfur powder is placed in the left-hand boat. The prepared layer is then placed inside the furnace, and the substrate is placed on the other side of the furnace in the opposite direction of the gas. MoO_3 and S are first evaporated at a specific temperature in the chemical vapor deposition method. The S vapor then passes MoO_3 through an inert gas such as argon. MoO_3 film is sulfurized in this case. MoS_2 layers are then synthesized at 850 °C for 20 min and formed on a SiO_2 substrate. After growth, many triangular shapes are seen on the substrate. The distribution of these triangles on the substrate is random (Fig. 3 (b)) [81,82]. Table 1 summarizes some synthesis techniques that are already known until now.

4. Functionalization of MoS_2 nanostructures

In order to improve the properties and create a specific performance of molybdenum disulfide nanostructures for different purposes, functionalization and surface modification strategies are proposed. Many attempts have been made to chemically and physically functionalize various molybdenum disulfide structures. Chemical functionalization is usually accomplished by creating new covalent bonds between the modifier and the substrate, while physical functionalization uses interactions such as electrostatic attraction between materials [97]. In the following, these methods have been analyzed in detail.

4.1. Covalent methods

In chemical functionalization, new covalent bonds between molecules and nanostructures of molybdenum disulfide are formed through defects and vacancies in the plane or edges of its crystal lattice. Potentially, both the sulfur and molybdenum atoms in the structure of MoS_2 will be able to form covalent bonds based on the type of surface-modifying agents [98].

Target molecules that contain sulfur functional groups such as thiols will be able to coordinate with molybdenum atoms in the MoS_2 lattice. Sideri et al. covalently functionalized both 1T and 2H structures of MoS_2 with dithiolenes via a green root employing bis(thiolate) salts as ligands (Fig. 4(a)) to coordinate with Mo atoms in the structure [99]. In this novel synthesis method, water is used as a solvent, and the mixtures were heated at 80 °C for 72 h. They showed that incorporating dithiolenes will induce the outstanding properties of these compounds, such as electrochemical and photochemical activity in the MoS_2 nanostructures.

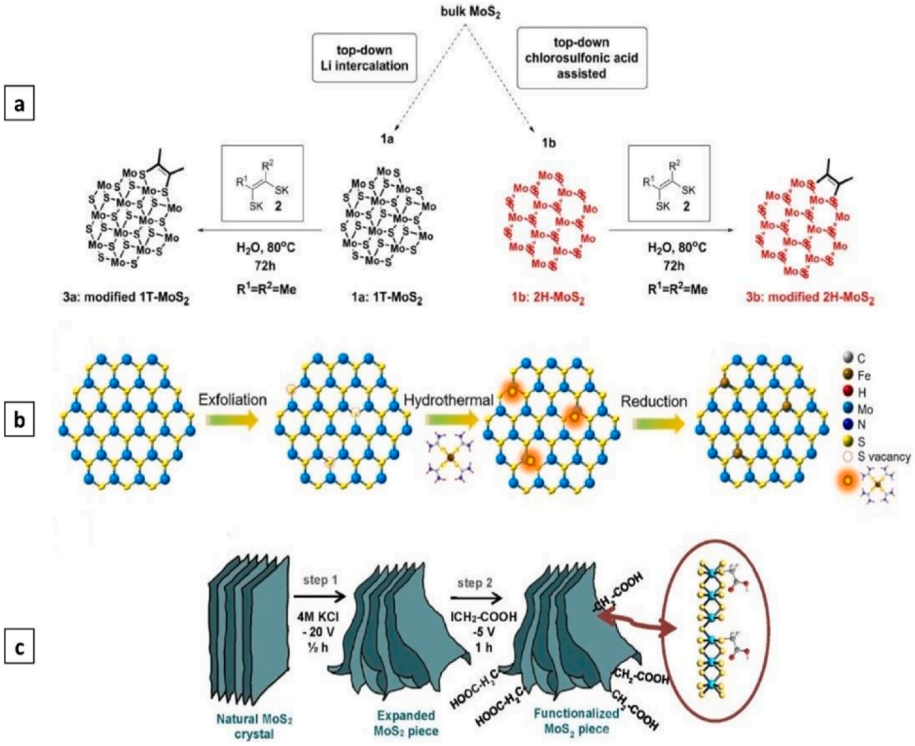

Fig. 4. Schematic illustration of various covalent MoS_2 functionalization approaches: (a) coordination of sulfur-containing functional groups to molybdenum atoms [99]; coordination of sulfur atoms on the structure of MoS_2 to a metal center containing modifier [103]; direct formation of C–S bond between MoS_2 and a reagent containing a carbon bonded to a leaving group [106].

Seo et al. employed the plasma method for generating more sulfur vacancies in the structure of MoS_2. They demonstrated that the resulting substrate was functionalized 1.8 times more than the conventional methods using 3-mercaptopropionic acid as a ligand [100]. Firstly, MoS_2 layers were generated on the surface of the Si/SiO_2 substrate by the chemical vapor deposition (CVD) method and then exposed for 2 s to the Ar^+ atmosphere to create more sulfur vacancies and more active sites for the subsequent reaction. Xu et al. prepared hyper-branched polyglycerol functionalized with lipoic acid and folic acid, attached it to the MoS_2 via covalent disulfide linkages, and subsequently loaded Chloroquine and doxorubicin drugs for targeted delivery to (HeLa-R) cells [101]. Lipoic acid acts as a bidentate sulfur ligand to bind the polymeric compound covalently to the structure of MoS_2 by simply mixing overnight at room temperature.

Modifiers containing metal centers will be able to coordinate with sulfur atoms in the structure of molybdenum disulfide. Liu et al. coordinated transition metals such as Au, Ni, Cu, Zn, Co, Mn, and Cr to the structure of molybdenum disulfide by immersing a CVD-grown MoS_2 on the Si/SiO_2 substrate into ethanolic solutions of the metal salts for 10 min [102]. They showed that these complexes significantly improve the electrical and optical properties of MoS_2. They exclusively deposited single gold atoms on the substrate via Au–S interactions. Zheng et al. loaded transition metals at the atomic level on molybdenum disulfide's surface (Fig. 4(b)) for further use as catalysts in petrochemical-related chemical transformations [103]. They added transition metals-thiourea complexes to the chemically exfoliated MoS_2 nanosheets, and subsequently, the self-assembled complexes were reduced to metal atoms under hydrothermal conditions. Chemical exfoliation employing n-BuLi causes negatively charged centers and, by creating strong interactions with metal complexes, prevents the accumulation of metal nanoparticles.

The direct C–S bond formation between sulfur atoms in the structure of molybdenum disulfide and carbon in organic compounds has also been reported. Daukiya et al. formed covalent C–S bonds on the surface of the MoS_2 using aryl diazonium chemistry [104]. They grafted 4-nitrobenzene diazonium tetrafluoroborate (4-NBD) on MoS_2 using potassium iodide as an activator. For this purpose, a substrate deposited with bulk MoS_2 was drop cast using an aqueous solution of 4-NBD and KI with a 1:1 M ratio. The iodide ions reduce the diazonium salt to the reactive 4-nitrophenyl radical that subsequently couples with the sulfur atoms existing on the substrate. Vera-Hidalgo et al. reported the attachment of maleimides to MoS_2 structure through Michael's addition reaction [105]. These maleimides act as mediators and enable the platform to perform subsequent reactions more easily. In this procedure, the bulk MoS_2 exfoliated in 2-propanol/water liquid phase using an ultrasonic probe device. Afterward, the solvent changed with acetonitrile and maleimides with different substitutions on the nitrogen atom, and triethylamine was added to the reaction flask. After 16 h, the functionalization reached 11–24 wt % of the substrate. Paredes et al. introduced a novel electrochemical-based functionalization of MoS_2 by applying a cathodic potential in the presence of organoiodides (Fig. 4 (c)) [106]. A piece of MoS_2 crystal as working electrode versus platinum foil as counter electrode in a two-electrode configuration was exfoliated by applying −20 V DC potential in 4 M KCl electrolyte for 30 min. Then the functionalization is accomplished by changing the electrolyte with the iodoacetic acid solution and applying a −5 V DC potential for 1 h. This electron supply from an external source causes nucleophilic addition of sulfur atoms to iodoacetic acid and substitution with iodine. These modified MoS_2 platforms were subsequently used to catalyze nitroarenes reduction reactions.

4.2. Non-covalent methods

Principal methods of non-covalent functionalization of molybdenum disulfide usually consist of depositing various mineral salts on MoS_2, forming its composites with other nanostructures using the ultrasonic method based on Van der Waals interactions, and creating electrostatic interactions with organic molecules. Mohapatra et al. grew a β-In_2Se_3 layer employing a two-step CVD method on the surface of MoS_2 and designed a hybrid-layered compound through Van der Waals forces [107]. This hybrid material showed promising characteristics for optoelectronic applications. Xie et al. physically modified the surface of MoS_2 with amphiphilic phospholipid to enhance its biocompatibility [108]. Lipid and molybdenum disulfide solutions were mixed in specific proportions in a shaker for 12 h at 37 °C and prepared after washing and centrifugation for drug loading. The resulting material showed good stability in biological environments and successfully delivered an anti-cancer drug to mice tumors. Zhang et al. functionalized negatively charged MoS_2 nanoflowers with cationic hydroxyethyl cellulose through electrostatic interactions [109]. An aqueous mixture of molybdenum disulfide and hydroxyethyl cellulose was sonicated in an ultrasonic bath followed by heating at 80 °C for 4 h. The resulting carrier is used for transdermal atenolol delivery under near IR irradiation.

4.3. Functionalized MoS_2 nanostructures for biomedical applications

The nanostructures used in biomedical fields, mainly used as substrates and scaffolds for carrying drugs and biological materials, should be biologically neutral and not stimulate the immune system or cause irritation at the application site [110]. Molybdenum disulfide surface functionalization approaches can be based on various factors such as the hydrophilic or hydrophobic nature of the transported drug, placing different chemical and biological receptors in order to deliver the drug specifically to the target site, placing compounds on it in order to neutralize it when exposed to the immune system, stabilizing it in physiological media, and so on [31]. These approaches can be implemented either by physical functionalization or by creating new chemical bonds, each of which has advantages and disadvantages. Creating new chemical bonds mainly requires the use of reagents and chemical mediators and toxic solvents, performing multi-step and time-consuming reactions, and precise purification processes. However, the high strength of the newly formed bonds can ensure the incorporation of new groups on MoS_2 nanostructures, which are primarily irreversible and do not separate from the surface. In contrast, creating physical interactions between materials is usually a simple process that takes place in a short time, and the residual materials are removed through washing. However, compared to chemical bonds, these interactions are generally not strong enough, and there is a possibility of separating nanocomposite components in different biological and chemical environments [97]. Linear polyethylene glycol (PEG) molecules are soluble in water and most organic solvents. Their hydrophilic nature and low toxicity have caused them to be used as structure-improving agents in drug delivery. Connecting polyethylene glycol chains to the surface of nanostructures (PEGylation) reduces their cytotoxicity and enzymatic digestion and increases their stability in biological environments by preventing their clumping [111]. PEGylation of MoS_2 nanosheets has been successfully performed with both covalent and non-covalent approaches for use in biomedical fields. Using sulfur chemistry, Liu et al. attached lipoic acid terminated PEG covalently to iron oxide decorated MoS_2 nanosheets. The resulting platform was subsequently radiolabelled with ^{64}Cu for multipurpose imaging and photothermal therapy in mice samples [112]. Malagrino and co-workers synthesized flower-like MoS_2 in the presence of PEG as the surface modifier and structure directing agent via the hydrothermal method. The simultaneous presence of polyethylene glycol and the precursors induces a specific morphology of molybdenum disulfide and modifies its surface through physical interactions. The addition of gold nanoparticles to this collection has created a platform with therapeutic and diagnostic applications [113]. Drugs as pharmaceutically active agents are essential components in the structure of nanocomposites used in targeted chemotherapy. In order to realize the controlled release of the drug at the desired location, most drug loading approaches on the surface of nanocarriers are limited to creating

intermolecular forces and electrostatic interactions. For instance, a platform based on functionalized MoS_2 nanosheets with folic acid and bovine serum albumin as targeting agents and PEG and polyethylene imine (PEI) as stabilizers was fabricated by zhang's group [114]. After fabrication of the platform, the aqueous dispersion of nanocomposite was added to the solution of doxorubicin (DOX). Subsequently, the drug was loaded via electrostatic interactions on the platform overnight (Fig. 5 (a)). In contrast, recently, a novel drug delivery platform was developed by Mo and coworkers in which the thiolated doxorubicin (SH-DOX) drug is attached to the molybdenum disulfide surface through the creation of covalent bonds [115]. This platform was further modified with PEG and a peptide for better dispersion and targeted delivery to Hela cells, respectively. The advantage of this method is the creation of strong bonds between the drug and the platform, which prevents unwanted release on the way to the target, and instead, a highly specific glutathione-stimulated release occurs through disulfide bond cleavage at the tumor site.

The covering cells of the body in sensitive parts such as the brain, placenta, and kidney are put together with strong connections like a barrier to prevent dangerous chemicals from entering the essential organs. By surface absorption of proteins such as immunoglobulin, albumin, and others, nanoparticles are integrated and form a mass. They enter the cells via various pathways of endocytosis and pinocytosis depending on the size of the mass and after attaching to receptors on the surface of the cell membrane [116]. Nanoparticles with a size of <100 nm can easily pass through cell membrane barriers like gas molecules, enter organs, tissues, cells, and even important organelles such as nucleus and mitochondria and deposit there. In comparison, larger nanoparticles are recognized by the body's immune system and are prevented from entering most tissues [117,118]. Because of fast vessel development, chaotic flows, and the unequal distribution of oxygen and nutrients, the endothelial cells of tumor blood vessels have irregular sizes and shapes, resulting in inter-endothelial cell gaps throughout the vessel wall. Depending on the type of cancer cells, the aforementioned gaps can be between 100 and 500 nm [119]. As a result, these factors should be taken into account while designing nanosystems for usage in the body. MoS_2 nanosheets can have dimensions of about 50 nm to 2 μm depending on the synthesis method [120], and various surface modifications can be applied for size tuning. For example, Liu et al. synthesized MoS_2 quantum dots with outstanding photoluminescent properties through the hydrothermal method with a mean hydrodynamic diameter of 4 nm. Next, due to the size requirements and reducing the toxicity effects of quantum dots and preventing those from entering healthy cells, by using glutaraldehyde mediators, polyethylene glycol with terminal amine groups have been connected to their surface through covalent bonding [121]. After PEGylation of MoS_2 quantum dots, the average size of the platform was evaluated to be 136 nm, which has the potential for employment as a drug delivery system (Fig. 5 (b)). Cell viability test using U251 cell line also demonstrated that MoS_2 quantum dots have more cytotoxicity than MoS_2-PEG.

5. Toxicity and biocompatibility of MoS_2

MoS_2 is easily functionalized due to its high surface area and interacts well with the environment. In each of the plates that make up the 1T-MoS_2, due to the lack of any hanging bonds, it does not react easily with the chemicals in the environment, which makes it highly stable in the surrounding environments, which makes these materials suitable for use in biological applications [122].

Recent research on targeted drug delivery systems for cancer therapy has focused on the use of MoS_2-based nanosheets for chemotherapy drug delivery. These nanosheets are expected to become as common as graphene quantum dots (GQDs) and graphitic-C_3N_4 QDs for oncological purposes.

A dose-dependent sulforhodamine B (SRB) assay was performed to evaluate the nano-toxicity associated with MoS_2 nanosheets. In this experiment, rat adrenal medullary endothelial cells (RAMEC) cells were incubated separately with MoS_2 nanosheets. The SRB assay measures the amount of protein in living cells to find the density of living cells [123]. To understand the effect of MoS_2 nanosheets on RAMEC and pheochromocytoma cells (PC12), electrochemical impedance spectroscopy (EIS) studies was performed to identify the cytotoxic effects of the synthesized MoS_2 nanosheets. The EIS system is a sensitive instrument for measuring cell resistance and electrode resistance changes that provide information about changes in cell density or morphology. The whole cell-based EIS system, previously reported by the group [124], is a sensitive and non-invasive approach to quantitative real-time measurement of cytotoxicity. In the study conducted by Liu et al., MoS_2 nanosheets were first added to the wells. Then, RAMEC cells were attached to the EIS chip. The change in resistance due to cell attachment to electrodes during the 50 h of the experiment showed that MoS_2 nanosheets are far superior for biological applications compared to their two-dimensional counterparts [125]. The lower cytotoxicity of the MoS_2 nanosheets synthesized in this work can be attributed to the fact that the edges of the MoS_2 nanosheets were not able to cut the cell membrane or penetrate to stress cell death [126]. Overall, from all previous reports, it is clear that these nanomaterials are excellent candidates for biological applications such as drug delivery, gene transfer, and bioimaging.

6. Drug delivery applications of MoS_2 nanocomposites

Cancer is one of the deadly diseases that kills many people yearly

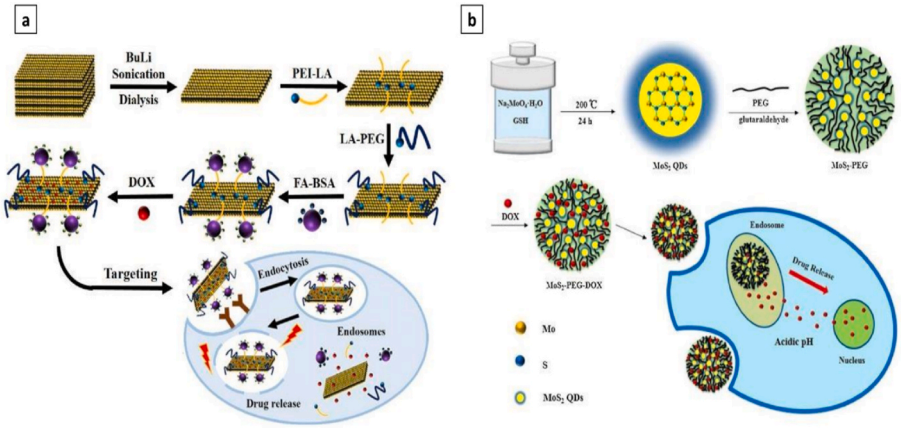

Fig. 5. schematic illustration of biomedical applications of functionalized MoS_2: (a) DOX loaded PEGylated MoS_2 nanosheets for targeted chemo-photothermal therapy [114]; (b) size tuning of MoS_2 quantum dots via PEGylation for pH-sensitive drug delivery [121].

[127–129]. For this reason, extensive research is conducted to find new methods and drugs to treat this disease [130–132]. In recent years, the development of a significantly reduced reactive drug delivery system (DDS) has received much attention. To this end, various biomolecules and DDSs have been synthesized by changing their environment as nanocarriers that respond to stimuli with respect to light, pH, magnetic field, ultrasound, and redox potential [133]. Two-dimensional materials are a group of materials that have attracted a lot of attention due to their unique physical and chemical properties. Transition metal dichalcogenides (TMDCs) are another class of two-dimensional materials with high potential for biological applications. Outstanding optical properties, the high specific surface area that makes them easily functionalized with biocompatible polymers, biomolecules or drugs, low toxicity, and high NIR light absorption are some of the properties that make these materials promising photothermal therapy candidates [134].

TMDCs are layered materials with the chemical composition MX_2, with M representing the central intermediate metal atom and X representing the atomic calcium (Te, Se, and S) atoms. These include MoS_2, WS_2, $MoSe_2$, and WSe_2 [135].

Kim et al. reported that by physiochemically altering the properties of delivery systems, they could be used to isolate the disulfide bond in the carrier for gene delivery and control the release of cargo at the target site [136].

Researchers have focused on stimulus-responsive multidirectional nanocarriers (smart DDSs) that can deliver drugs in response to internal or external stimuli such as pH, redox, temperature, enzyme, magnetic, and light (release into the environment).

For instance, a cystamine–glutathione- molybdenum disulfide-Pluronic F127 (CYS-GSH-MoS_2-PF127) nanocomposite was synthesized for effective drug delivery in a glutathione-rich environment. To prepare these nanocomposites, MoS_2 was first separated by an ultrasonic process using GSH as a surfactant, then a solid containing CYS was added. Finally, PF127 was introduced to extract GSH-responsive MoS_2-GSH-CYS-PF127 nanocomposite. The MoS_2 nanocomposite system in the GSH medium was validated by TEM and DLS [114,137]. Drug release was dependent on GSH reduction with changes in pH and evaluated by a phosphate buffer at pH 7.4 and GSH = 5 mM. After 72 h, 52% of the drug was released. Also, HeLa cells were used as a model cancer cell line to study the effect of the fabricated drug carrier. According to fluorescence microscopic images, incubation of MoS_2 nanocomposites for 2 and 4 h showed the presence of the nanocomposites just in the cytoplasm of cells. Still, after 6 h, DOX was released from the nanocomposites and entered the nucleus of the cells. Thus, this MoS_2 nanocarrier opens up a promising path for use as a stimulus-responsive nanocarrier for drug delivery (Fig. 6) [137,138].

MoS_2 can be used as a nanocarrier functionalized with PEG or its analog for delivering chemotherapy drugs. Liu et al. first synthesized MoS_2 QDs through a hydrothermal process. They functionalized the unstable MoS_2 QDs prepared by oligomeric PEG terminated with diamine by covalent bonding in a physiological medium, cross-linked by a glutaraldehyde agent. The anticancer drug doxorubicin (DOX) was loaded onto MoS_2-PEG via a non-covalent bond, producing the nanoassembly of MoS_2-PEG-DOX. As a prerequisite for drug delivery and cell imaging, PEG deposition contributes to good biocompatibility, excellent physiological stability of MoS_2 nanocomposites, and reduction of DOX side effects on normal cells [121].

7. Application of MoS_2 in photothermal treatment for cancer therapy

Nanotechnology has opened a new window in cancer therapy using photothermal therapy by introducing nanostructures that absorb light and convert it into heat [139]. If used concurrently with common cancer treatments, photothermal treatment can significantly increase the effectiveness of treatment and reduce the side effects attributed to common cancer therapy options. Photothermal therapy (PTT) is one of these treatments that is less invasive than other treatments because water molecules, melanin, and hemoglobin, which are the essential factors in absorbing light exist in the body. For this reason, photothermal therapy has gained attention as a viable option for cancer treatment, particularly when combined with other treatments [140].

For effective treatment using high efficiency photothermal method, the presence of light to heat conversion factor is essential. In nanometer-sized photothermal exchangers, the thermal photo capacity depends on the increase in surface plasmon resonance (SPR), which occurs due to increased fluctuations in the free electrons of the nanoparticle surface due to light irradiation. In this process, nanoparticles can scatter or absorb light [141]. The light absorption by nanoparticles excites free electrons at their surface, which can be returned to lower energy levels by emitting light (luminescence) or releasing heat. In the thermal photo phenomenon, nanoparticles with high absorption and low luminescence can have the most efficient conversion of light into heat. Therefore, the efficiency of nanoparticles in converting light into heat must be considered in photothermal therapy applications. So far, much research has been done to find an influential factor in photothermal treatment that has high efficiency and does not cause toxicity to the body. The optical properties of MoS_2 depend on the number of layers of this material. For example, the MoS_2 bulk sample has an indirect energy gap,

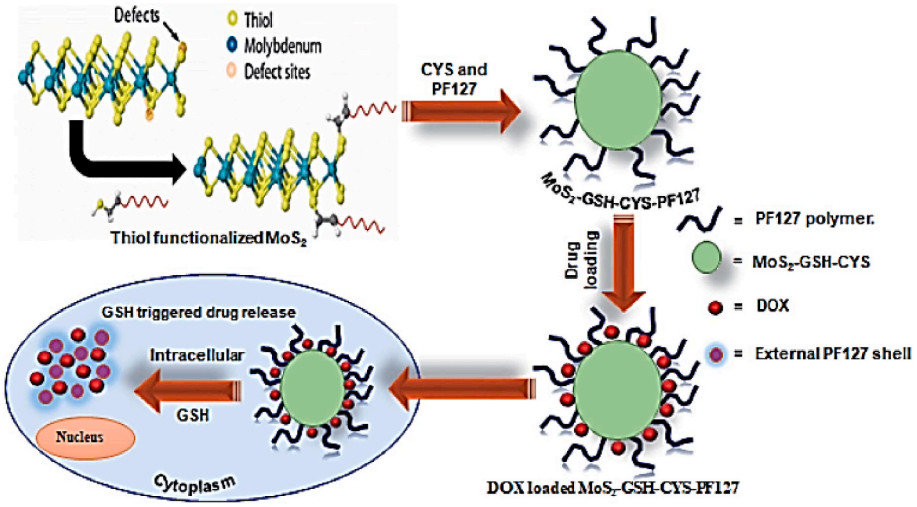

Fig. 6. Schematic illustration of the synthesis of DOX-loaded MoS_2–GSH–CYS–PF127 nanocomposites for GSH reduction-responsive drug release [137].

while the energy gap for the monolayers of this material is of the direct type [142]. So, photons are easily absorbed by the MoS_2 monolayer, which has more energy than the energy gap. Also, light absorption depends on exciting transmission due to the strong interaction between electrons and holes.

Many groups in the last decade have studied MoS_2 due to their high surface-to-volume ratio, high light-to-heat conversion, biocompatibility, and optical stability as suitable photothermal converters for treating cancerous tumors.

The main limitation of MoS_2 as a nanostructure for drug delivery applications is its low stability in biological environments as an influential factor in biomedicine. In order to overcome this limitation, these nanoparticles have been surface-modified with various biocompatible polymers and molecules in water [143].

Choe and colleagues first claimed in 2013 that two-dimensional MoS_2 nanostructures are effective agents in photothermal therapy that can be more efficient than gold nanoparticles, graphene, and its derivatives. According to the group, MoS_2 has an extinction coefficient of 29.2 nm $Lg^{-1}.cm^{-1}$ at 800 nm, while the extinction coefficient reported for graphene oxide (GO) $Lg^{-1}.cm^{-1}$ is 3.6. For most gold nanorods, $Lg^{-1}.cm^{-1}$ is 13.9 and for reduced graphene oxide (rGO) is about 24.6 $Lg^{-1}.cm^{-1}$ [144].

In order to increase the penetration of nanostructure into cells and make the treatment more effective, combining two methods of photothermal therapy and photodynamic therapy has been one of the options studied by researchers. According to research by Liu et al. [145], nanoparticles coated with polyethylene glycol (MoS_2-PEG) can act as a photothermal converter and a carrier for Chlorin e6 (Ce6), an effective factor in photodynamic therapy, and cause a significant increase.

In other studies simultaneously performed by the same group, MoS_2 nanoparticles were functionalized by polyethylene glycol (PEG), and then folic acid was attached to the structure. PEG polymer plays two roles here. First, it increases the biocompatibility of nanoparticles and, at the same time, leads to the binding of folic acid for targeted entry into cancer cells [146]. They reported complete tumor removal using NIR imaging performed well with nanofibers and controlled release of doxycycline. The team continues their research on MoS_2-PEG nanostructure with iron oxide superparamagnetic nanoparticles and PTT treatment and PAT imaging, positron emission cross-section (PET), and magnetic resonance imaging (MRI).To use the imaging of PET nuclei, they used copper ions 64, which can be readily adsorbed in places with a defect of molybdenum atom and bond with sulfur atom without the need for any intermediate molecule to bond [147]. The two-dimensional platform was tested on mice infected with 4T1 cells. 808 nm laser irradiation resulted in complete tumor removal, while triple imaging made it easy to track the nanostructure and examine the tumor. This nanostructure confirms the use of intermediate metal dichalcogenes as multiple diagnostic-therapeutic substrates [33].

In the same year, Wang and colleagues tested another compound (MoS_2/Bi_2S_3-PEG). This combination has high colloidal stability and biocompatibility for PTT treatment combined with CT and PA imaging. Bismuth (Bi) has an increased ability to absorb X-rays, leading to this substance's widespread use in CT imaging and cancer treatment with radiotherapy (RT). X-ray bismuth atoms exhibit strong photoelectric properties so that when exposed, they can effectively break DNA strands by producing secondary electrons, resulting in damage and death of cancer cells [148].

Polyvinyl pyrrolidone (PVP) is another polymer that has been studied for surface modification and enhanced biocompatibility of MoS_2 nanoparticles. This polymer acts as a surfactant and as a nanoparticle size controller. The molecular weight of PVP used is a critical parameter in determining the size and morphology of nanoparticles [5,149].

The shape of the resulting nanoparticles when PVP with a molecular weight of 360 kDa is used, with very small sizes of 4.4. 4.21 nm, and when PVP with a molecular weight of 30 kDa is used, it is entirely uniform. Due to the short polymer chains, the limiting forces for nanoparticle growth were weak and insufficient, resulting in the growth of nanoparticles in which impure phases were observed. Also, when a polymer with a molecular weight of 360 kDa was used, doubling the polymer concentration resulted in the production of 2.1 $\pm$ 7.14 nm nanoparticles [150].

According to the good and promising results obtained in the field of cancer treatment with photothermal therapy and its combination with other methods, researchers are looking for solutions in addition to the mentioned cases to be able to deliver drugs to the tumor site in a targeted manner.

One of the successful nanosystems developed for this purpose is MoS_2-PEI-HA. MoS_2 was decorated with hyaluronic acid (HA) in this study using polyethyleneimine (PEI). The application of HA in developing this platform serves two functions. First, it facilitates the targeted delivery of doxorubicin (DOX) to drug-resistant MCF-7-ADR cells. Second, HA is degraded by hyaluronidase (HAase), which is an enzyme accumulated in the tumor microenvironment and increases the release of DOX. On the other hand, MoS_2 also increases the release of the drug into the cell environment due to its high ability to absorb light with a wavelength of 808 nm. The combined photothermal property of MoS_2 and enhanced targeting of breast cancer cells with HA reduces p-glycoprotein (P-gp) gene expression, which enhances drug uptake and reverses drug resistance [151].

Another similar method recently published is the synthesis of MoS_2-HA-DTPA-Gd/Gef nanostructure. In this nanostructure, MoS_2 was functionalized with hyaluronic acid (HA) for enhanced targeted delivery of gefitinib (Gef) due to the binding of HA to the CD44 receptor. The fabricated platform was also loaded with contrast agents based on gadolinium (Gd) for magnetic resonance imaging (MRI). In addition, the photothermal attribute of MoS_2 resulted in tumor ablation of A549 and H1975 under NIR [152].

Table 2 examines several most recent molybdenum disulfide-based drug delivery and photothermal therapy platforms.

8. Functionalized MoS_2-Based nanomaterials for tissue regeneration

One of the critical research fields of tissue engineering and clinical challenge for nanotherapy is the functionalization of MoS_2-based nanomaterial for tumor tissue regeneration and paracarcinoma tissue. Recently, a study on the treatment of malignant bone tumors and normal tissue regeneration was done by making bifunctional 3D printed scaffolds via a hydrothermal path. MoS_2 nanosheets were attached to the surface of 3D-printed akermanite ($(Ca_2MgSi_2O_7)$ AKT) bioceramic scaffolds, followed by in situ growth of MoS_2 nanosheets on the surface of AKT scaffolds offering photothermal attribute to the MS-AKT scaffolds. The temperature of MS-AKT scaffolds increased significantly due to the photothermal effect of MoS_2 inhibiting the viability of Saos-2 cells (osteosarcoma cells) and MDA-MB-231 cancer cells in vitro and in vivo. In addition, the scaffolds facilitated the rapid proliferation of mesenchymal stem cells and bone differentiation, thus facilitating bone regeneration, healing, and bone growth as the second function of the developed scaffolds [206].

Similarly, MoS_2 composite nanofibers were recently prepared by electrospinning technology and a doping method for biocompatibility measurement and bone marrow mesenchyme stem cells (BMSCs) proliferation detection [207]. Consequently, enhanced BMSC growth rate and cellular activity by fabricating electrospun poly(ε-caprolactone)/-molybdenum disulfide composite nanofibers indicate improved osteogenesis. Simultaneously, the alkaline phosphatase (ALP) content significantly increased as the MoS_2 nanofiber concentration increased. These phenomena suggest that as-prepared MoS_2 composites pave a new way for applying well-defined nanostructure materials into tissue engineering [31].

Not limited to bone engineering, MoS_2 nanosheets are also favorable structures for cardiac tissue regeneration because they can imitate

Table 2
Most recent MoS_2-based platforms for drug delivery and photothermal therapy.

Platform	Application	Drug/Primary therapy	Additional therapy	Highlights	Year	Ref.
Magnetic MoS_2/ polymeric dendrimers/L-arginine	Chemo-photothermal therapy of cancer cells	Cisplatin	Photothermal therapy	pH and temperature-responsive release of cisplatin was achieved. Increasing temperature and decreasing pH increased cisplatin release with 86% and 92% at pH 7.4 and 5.6, respectively.	2020	[153]
MoS_2/1-tetradecanol	Chemotherapy with photothermal stimuli for drug release	Doxorubicin	Photothermal stimuli	The platform showed photothermal release of doxorubicin and effective killing of HepG2 liver cancer cells.	2020	[154]
Polyacrylamide/MoS_2	Transdermal drug delivery with photothermal conversion	Atenolol	Photothermal conversion	The platform is used for transdermal atenolol delivery. Also, the composite showed high photothermal conversion efficiency.	2020	[155]
Poly (acrylic acid)/MoS_2	Transdermal drug delivery	Atenolol	Photothermal conversion	This delivery system provides significant loading capacity for atenolol as a novel method for hypertension treatment through transdermal delivery. Also, this platform represented controlled drug release with improved skin penetration by skin laser irradiation.	2020	[156]
L-cysteine/MoS_2 (MoS_2/ Cys)	Photothermal therapy of cancer cells	Photothermal therapy	————	This biocompatible platform shows high photothermal conversion efficiency under laser irradiation and inhibits cancer cell growth by internalizing developed nanospheres in Hep G2 cells.	2020	[157]
MoS_2/PEG/ polydopamine/ Aptamer	Chemo-photothermal therapy of cancer cells	Doxorubicin	Photothermal therapy	The aptamer was used to create specific interactions with MCF-7 breast cancer cells. The platform was loaded with doxorubicin and accelerated drug release under laser irradiation and lysosomal acidic condition. The presence of MoS_2 and polydopamine (PDA) causes hyperthermia for killing cancer cells.	2020	[158]
Fluorescein isothiocyanate/MoS_2/ Mesoporous silica nanoparticles (MSN)	Fluorescence imaging and photothermal therapy	Photothermal therapy	Fluorescence imaging	The platform showed a photothermal effect under laser irradiation and imaging capability after conjugating fluorescein isothiocyanate (FITC) with MSN by amide bonds.	2020	[159]
MoS_2/Glucose oxidase/ Sodium alginate/Fe^{3+} hydrogel (MAF)	Tumor starvation, photothermal, and chemodynamic therapy	Starvation therapy through consuming glucose to produce hydrogen peroxide (H_2O_2), followed by a redox reaction to produce Fe^{2+} from MoS_2 to form Fe^{3+}	Induction of a Fenton reaction to continuous conversion of H_2O_2 to hydroxyl radicals for the chemodynamic therapy as well as the photothermal effect of MoS_2	The MAF hydrogel restricts the glucose availability for cancer cells and causes starvation. Also, the hydrogel exhibits high photothermal conversion under laser irradiation. The presence of Fe^{2+} ions causes Fenton reaction to destroy HT 29 cancer cells.	2020	[160]
FeO/MoS_2/bovine serum albumin	Chemodynamic and photothermal therapy of cancer cells	Chemodynamic therapy	Photothermal therapy	The photothermal effect of MoS_2 combined with the Fenton reaction induced by Fe ions resulted in effective and synergistic in vivo cancer treatment.	2020	[161]
Chitosan/MoS_2	Antibiotic and photothermal therapy of bacterial infections	Antibiotic therapy of *Staphylococcus aureus*	Photothermal therapy at mild temperature	The platform is loaded with ofloxacin antibiotic and causes local hyperthermia under laser irradiation. No damage to adjacent tissues was observed due to the operation at mild temperatures with low concentrations of antibiotics.	2020	[162]
MoS_2/Cu^{2+}	Photocatalytic and photothermal therapy of *Staphylococcus aureus* bacterial infections	Photocatalytic therapy by rapid transfer of electrons from the conduction band of MoS_2 to copper ions, which improves ROS production yield	Photothermal therapy due to the photothermal potential of MoS_2, which enables absorbing photons and converting photoenergy to heat	Cu^{2+} ions enhance the photothermal conversion efficiency of MoS_2 nanosheets. The platform showed excellent antibacterial efficiency under visible light irradiation.	2020	[163]

(*continued on next page*)

Table 2 (*continued*)

Platform	Application	Drug/Primary therapy	Additional therapy	Highlights	Year	Ref.
MoS_2/Carbon nanosphere	Chemo-photothermal therapy of cancer cells	Doxorubicin	Photothermal therapy	High anti-cancer drug loading capacity and excellent photothermal conversion under laser irradiation were achieved. Based on the in vitro evaluations, the platform releases the model drug in response to pH, temperature, and NIR changes.	2020	[164]
Polypeptide/MoS_2	Photodynamic, chemotherapy, and photothermal therapy of 4T1 breast cancer cells	Doxorubicin	Photothermal and photodynamic therapy	This injectable and biocompatible hydrogel is loaded with doxorubicin for the synergistic treatment of cancer cells. Excellent photothermal properties due to the presence of MoS_2 were realized.	2020	[165]
TaO_2/Chitosan/MoS_2	Photothermal therapy of breast cancer cells (MCF-7)	Photothermal therapy	———————	Tantalum oxide improved the photothermal properties of MoS_2 nanosheets by improving photothermal conversion efficiency, biocompatibility, and photostability. Thus, this platform opens a new avenue in biological features for photothermal cancer therapy.	2020	[166]
Phospholipid/MoS_2	Chemo-photothermal therapy of cancer cells	Doxorubicin	Photothermal therapy	Phospholipids improved the stability and biocompatibility of MoS_2 in a biological medium. Good photothermal conversion efficiency, improved drug loading efficiency, and pH-dependent release were observed.	2020	[108]
MoS_2/PEG/Erlotinib/ Doxorubicin	Chemo-photothermal therapy of cancer cells	Doxorubicin temperature-sensitive release by absorbing NIR and sensitizing lung cancer cells (A549) by erlotinib (Er) toward apoptosis induction	Photothermal therapy	This platform converts laser irradiation to heat and releases the doxorubicin in a controlled manner. After the uptake of the platform, erlotinib sensitized cells for apoptosis induction by DOX to realize a chemo-photothermal therapy.	2020	[167]
Hyaluronic acid/ Polyethyleneimine/ PEG/MoS_2	Targeted chemo-photothermal therapy of cancer cells	Doxorubicin	Photothermal therapy	This platform delivers the doxorubicin specifically to MCF-7breast cancer cells in vitro by a dual responsive behavior (pH and NIR) and inhibits tumor growth in breast cancer model of mice. Loading melanin onto the MoS_2 increases the photothermal properties of the nanocomposite. Moreover, hyaluronic acid (HA) facilitates targeting cancer cells due to the interaction of HA with CD44 receptors.	2020	[168]
Metal organic framework (MOF)/ polydopamine/ hyaluronic acid/MoS_2	Imaging, chemo-photothermal combined therapy	Doxorubicin hydrochloride	Photothermal therapy	The nanocomposite utilizes for cancer treatment and diagnosis. NIR and pH-responsive drug release accomplished targeted delivery of doxorubicin to cancer cells.	2021	[169]
Chitosan/MoS_2/Ag	Concurrent antimicrobial and anti-cancer activities	Antimicrobial activity	Anti-cancer effect	The platform was fabricated by liquid exfoliation. Due to containing Ag nanoparticles, the nanocomposite shows antibacterial properties toward various microorganisms. Furthermore, the platform offers cytotoxic activity toward MCF-7 breast cancer cells.	2021	[170]
Poly (ethylene glycol)/ triphenyl phosphonium/ polydopamine/ Fe^{3+}coated MoS_2	Photodynamic-chemodynamic oncotherapy	Targeting mitochondria of cancer cells by producing hydroxyl radicals	Photothermal-chemodynamic therapy	Mitochondria targeted photothermal activity under the near-IR region for destroying 4T1 cancer cells	2021	[171]
Mg/Mn/Al double hydroxides clay/ MoS_2/bovine serum albumin	Imaging and tumor phototherapy	Doxorubicin	Photodynamic therapy with ROS production through catalyzed decomposition of H_2O_2 by LMM@BSA	Combination of photothermal properties of MoS_2 with the catalytic activity of clay for effective cancer treatment	2021	[172]

(*continued on next page*)

Table 2 (*continued*)

Platform	Application	Drug/Primary therapy	Additional therapy	Highlights	Year	Ref.
Gambogic acid/MoS_2/bovine serum albumin/Gd_2O_3/hyaluronic acid	Low-temperature photothermal therapy (LTPTT) and chemotherapy	Gambogic acid (GA)	Chemotherapy	One-pot platform preparation for magnetic resonance imaging and effective photothermal therapy for killing MDA-MB-231 breast cancer cells at a mild temperature was realized in this study.	2021	[173]
MoS_2/Au nanorods	Synergistic photodynamic-photothermal therapy for antibacterial disinfection	Photodynamic therapy	Photothermal therapy	Increase in temperature and creation of reactive oxygen species (ROS) under laser irradiation for employing against E. coli bacteria	2021	[174]
MoS_2 nanoflakes	Drug delivery and photothermal therapy	Erythromycin	Photothermal therapy	Good drug loading capacity and controlled release of erythromycin with NIR were achieved for topical delivery with a sustained flux through the skin.	2021	[175]
Poly [N-Vinyl caprolactam-co-Vinyl Acetate] copolymer/MoS_2/3, 4-diamino-benzoic acid	Drug delivery and photothermal therapy	Imatinib Mesylate (IM)	Photothermal therapy	Photosensitive release of imatinib mesylate as an anti-cancer drug due to shrinkage of polymer chains by increasing the temperature was achieved.	2021	[176]
Polyvinyl alcohol (PVA)/gum tragacanth (GT)/MoS_2	Drug delivery	Tetracycline (TCH)	————————	This nanofiber exhibits an inhibitory effect on gram + bacteria, including *Staphylococcus epidermidis*, *Bacillus subtilis*, and *Staphylococcus aureus*, and *Escherichia coli* and *Pseudomonas aeruginosa* as Gram-negative bacteria. Also, controlled release of tetracycline was achieved after the inclusion of MoS_2 in the nanocomposite.	2021	[177]
β-cyclodextrin/MoS_2	Antimicrobial and anti-cancer activities	—————	————————	The functionalized MoS_2 with β-cyclodextrin demonstrated an excellent growth inhibition on bacteria like *S. aureus* and *E. coli* and cancer pathogens, particularly the MCF-7 cancer cell line.	2021	[178]
MoS_2 nanodots/mesoporous silica nanospheres	Cancer therapy and imaging	Doxorubicin	Cancer imaging of breast cancer and glioma	Functionalized mesoporous silica nanospheres with MoS_2 nanodots result in the pH-responsive release of DOX based on the electrostatic interactions and is a good contrast agent for CT imaging of breast and glioma cancer cells.	2021	[179]
N- isopropyl acrylamide/polyethylene glycol/MoS_2	Chemo-photothermal therapy of cancer cells	Doxorubicin	Photothermal therapy	This biocompatible and thermo-sensitive platform showed DOX adsorption and release with an acceptable photothermal activity under near IR irradiation with improved apoptotic induction compared to monotherapy.	2021	[180]
Polyglycerol functionalized MoS_2	Chemo-photothermal therapy of cancer cells	Doxorubicin and chloroquine	Photothermal therapy	This work developed a biocompatible pH and photothermal-responsive platform for the co-delivery of doxorubicin and chloroquine to destroy HeLa-R cells with excellent drug loading capacity.	2021	[101]
MoS_2/Carbon nanoparticles/PEG	Chemo-photothermal therapy of cancer cells	Doxorubicin	Photothermal therapy	Higher heat production after incorporating carbon in the nanocomposite. Controllable doxorubicin release by near IR irradiation and reducing pH from 7.4 to 5.	2021	[181]
Fe_3O_4/MoS_2/poly (N-vinyl caprolactam) (PNVCL)	Photothermal Drug release	Curcumin	————	The curcumin-loaded platform releases 100% of curcumin under near IR laser irradiation within 10 min. An increase in temperature due to the thermo-sensitive attribute of poly (N-vinyl caprolactam) increased drug release from 45% to 95% during 5 h.	2021	[182]

(*continued on next page*)

Table 2 (*continued*)

Platform	Application	Drug/Primary therapy	Additional therapy	Highlights	Year	Ref.
MoS_2/lipoic acid	Chemo-photothermal therapy of cancer cells	Hydroxycamptothecin (HCPT)	Photothermal conversion	Anti-cancer drug hydroxycamptothecin is loaded on the platform via ester linkages with a more stable connection than physical adsorption. The drug is selectively released in the presence of esterase.	2021	[183]
Lentinan functionalized MoS_2	Synergistic chemo-photothermal therapy of cancer cells	Gemcitabine (GEM)	Photothermal therapy	The developed platform is a suitable carrier for gemcitabine anti-cancer drug delivery with excellent light absorption capacity for dual pH and NIR-sensitive release behavior.	2021	[184]
MoS_2/perfluorohexane/ poly (lactic-co-glycolic acid)	Computed tomography (CT) imaging and photothermal therapy	Tumor ablation by photothermal conversion	Enhanced ultrasound/ computed tomography imaging	MoS_2 nanodots enhance the photothermal properties of the platform and its imaging capability.	2021	[185]
Polyethyleneimine/ Lipoic acid-modified poly (ethylene glycol)/MoS_2	Combined gene, chemo-photothermal therapy of cancer cells	Doxorubicin and siRNA	Photothermal therapy	The delivery system demonstrated pH and photothermal dependence release of doxorubicin and siRNA from the platform with synergistic healing of DOX-resistant MCF-7/ ADR cancer cells.	2021	[186]
PVA/MoS_2/Doxorubicin	Chemo-photothermal therapy of cancer cells	Doxorubicin	Photothermal therapy	The platform shows photothermal activity by converting light at 808 nm to heat. Also, the NIR irradiation increases the drug release rate for HT29 colorectal cancer treatment.	2021	[187]
MoS_2/polydopamine/ methoxy-polyethylene glycol (PEG)-amine	Chemo-photothermal-immunotherapy, and imaging	Cisplatin (Pt) and 1-methyl-tryptophan (1-MT)	Photothermal therapy and 1-MT-induced immune checkpoint blockade to generate T cells leading to the enhanced immune response against cancer.	The platform possessed simultaneous load and release of cisplatin and 1-methyl-tryptophan cancer drugs with high light to heat conversion efficiency for photo-sensitive drug release, pH-dependent drug release, computed tomography (CT), and photoacoustic imaging ability.	2021	[188]
PEG-modified MoS_2/ CeO_2	Photothermal, antibacterial, and antioxidant treatment of chronic wounds	Photothermal therapy	Antibacterial activity of MoS_2 modified by polyethylene glycol and the antioxidant activity of cerium dioxide nanoparticles	The combination of photothermal properties of MoS_2 with the antioxidant activity of CeO_2 nanoparticles made the platform an excellent candidate for treating diabetic wounds by removing ROS.	2021	[189]
MoS_2/Eu^{3+}	Photothermal-photodynamic therapy of 4T1 cancer cells	Photothermal therapy	Photodynamic therapy	The fabricated nanocomposite showed enhanced photothermal conversion efficiency (PCE) due to the presence of the europium ions (Eu^{3+}) for destroying cancer cells. Besides, Eu^{3+} promoted ROS production, which facilitates photodynamic therapy concurrently.	2021	[190]
Cu_2O/MoS_2	Synergistic chemodynamic (CDT) photothermal therapy (PTT) of cancer cells	Chemodynamic therapy (CDT)	Photothermal therapy (PTT)	The nanocomposite causes a Fenton-like reaction under laser irradiation and enhances the PTT effect due to functionalizing MoS_2 with Cu_2O as a transition metal ion to produce hydroxyl radicals.	2021	[191]
MoS_2/chlorine e6-Hyaluronic acid	fluorescence imaging and photodynamic-photothermal therapy of bacterial infections	Photothermal and photodynamic therapy	Fluorescence imaging (FLI)	Chlorine e6 (Ce 6) was utilized as a photo-sensitizer and a fluorescent probe conjugated with MoS_2 as a photothermal agent. The platform kills more than 99% of bacteria in infected tissues.	2021	[192]
MoS_2/bovine serum albumin/Aptamer	Targeted photothermal therapy of cancer cells	Photothermal therapy	————	The platform has good recognition capability to target tumor cells. Moreover, this biocompatible platform selectively kills breast cancer cells under laser irradiation, confirmed by in-vivo tumor-bearing mice analysis.	2021	[193]
PEG/MoS_2/BNN6	Antibacterial and antifungal photothermal therapy	Antibacterial and antifungal effects on *S. aureus* and *Candida*	Photothermal therapy at low temperature	MoS_2 nanoflowers were grafted with PEG to increase biocompatibility and loaded with	2021	[194]

(*continued on next page*)

Table 2 (*continued*)

Platform	Application	Drug/Primary therapy	Additional therapy	Highlights	Year	Ref.
		albicans with nitric oxide (NO) release		nitric oxide donor BNN6. The platform enhanced the loading efficiency of BNN6 due to the monolayer nanoflower structure of PEG/MoS_2. Under laser irradiation, the platform causes hyperthermia and releases NO for treating bacterial and fungal infections as a promising treatment compared to monotherapy.		
Indocyanine Green-Curcumin/MoS_2 Hollow Spheres	Photothermal therapy of cancer cells with enhanced photodynamic therapy	Photothermal therapy using Indocyanine Green (ICG)	Enhanced photodynamic therapy with P-gp expression inhibition using curcumin	Indocyanine Green acts as a photosensitizer, and curcumin inhibits p-glycoprotein, which can pump the drugs out of cancer cells.	2021	[195]
MoS_2/CuO/bovine serum albumin/imiquimod	Imaging, and synergetic photothermal therapy, chemodynamic therapy, and immunotherapy of cancer cells	Synergetic photothermal therapy, chemodynamic therapy, and immunotherapy	Computed tomography/infrared thermal/magnetic resonance (CT/IR/MR) multi-mode imaging	CuO semiconductor shows peroxidase-like behavior under laser irradiation and temperature increase caused by MoS_2 nanosheets. Imiquimod modifies anti-cancer immune responses to destroy the tumors through the combination of tumor-associated antigens and imiquimod (R837).	2021	[196]
MoS_2/poly dopamine/(5-carboxypentyl) Triphenyl phosphonium bromide	Chemo-photothermal therapy of cancer cells	Doxorubicin	Photothermal therapy	The nanocomposite is loaded with doxorubicin, and the photothermal effect causes up to 50°c hyperthermia to effectively kill A549 cancer cells. Dual stimuli-responsive drug release was applied based on the platform's pH and near-infrared light-responsive attributes.	2022	[197]
Magnetic MoS_2/Lipid	Chemo-photothermal therapy of cancer cells	Doxorubicin	Photothermal therapy	Doxorubicin loading efficiency and photothermal properties were improved. Modifying the platform with lipid enhanced drug accumulation at the tumor site. Cytotoxicity on MCF-7 cells was dependent on concentration.	2022	[198]
MoS_2/Tannic acid/Fe multifunctional hydrogel	Photothermal therapy of bacteria-infected wounds	Antibacterial activity due to enzyme activity	Photothermal therapy	The hydrogel showed anti-oxidant and anti-inflammation properties in addition to fast self-healing. Owing to catalase (CAT)-like activity, the platform decomposed H_2O_2 to O_2 to alleviate hypoxia and supply sufficient O_2. Also, GSH loss and the peroxidase (POD) activity contribute to the antibacterial feature of the hydrogel.	2022	[199]
Prussian blue (PB)/$Cu2^{+}$/Mn^{2+}/MoS_2/poly ethylene glycol	Magnetic resonance imaging (MRI) and chemo-photothermal therapy	Doxorubicin hydrochloride	Photothermal therapy (PTT)/chemodynamic therapy (CDT)	Excellent photothermal efficiency due to the presence of MoS_2 and suitable for chemodynamic therapy through catalytic properties Improved hypoxia of tumor microenvironment (TME) by reacting with H_2O_2 to generate O_2 and improve the chemotherapy effect of released DOX	2022	[200]
MoS_2/C/SiO_2	Chemo-photothermal therapy of cancer cells	Doxorubicin	Photothermal therapy	pH and NIR-responsive core-shell nanospheres are synthesized through the one-step hydrothermal method. Significant photothermal properties, high doxorubicin loading efficiency, and release ability inhibit 74.18% of MCF-7 breast cancer cells.	2022	[201]
MoS_2/TiO_2 nanofibers	Photodynamic-photothermal antibacterial therapy	Antibacterial activity	Synergistic effect of oxidase-like antibacterial activity along with photodynamic and photothermal therapy	Visible light and near-IR irradiation induce a photothermal effect and oxidase-like activity to relieve bacterial infections.	2022	[202]
MoS_2/Indocyanine green/Ag		Silver (Ag) applied as a chemical antibacterial agent	Chemotherapy, photothermal and photodynamic therapy	The platform acts as three modal antibacterial agents under laser	2022	[203]

(*continued on next page*)

Table 2 (*continued*)

Platform	Application	Drug/Primary therapy	Additional therapy	Highlights	Year	Ref.
	Chemo-photothermal-photodynamic antibacterial therapy			irradiation. Loading ICG and AgNPs increase the heat to achieve a combined or even synergistic effect.		
MoS_2/CNT multifunctional hydrogels	Photothermal wound disinfection	Antibacterial disinfection	Photothermal therapy	Peroxidase-like activity and free radical capturing properties of the hydrogels for wound healing are the features of this platform.	2022	[204]
MoS_2 quantum dots/ poly ethylene glycol/ folic acid	Chemo-photodynamic therapy of cancer cells	Doxorubicin	Photodynamic therapy	MoS_2 quantum dots are outstanding photosensitizers that can be activated by light to generate ROS. The fabricated platform alleviates the limited application of MoS_2 quantum dots due to the low penetration of visible light to tissues by converting NIR to visible light. Also, this nanoplatform enhanced the loading capacity of doxorubicin with a pH-responsive drug release.	2022	[205]

extracellular matrix and display electrical conductivity. After synthesis and infusion of MoS_2 materials to nylon6 electrospun nanofibers (Nylon/MoS_2 nanofibers), the composite can remarkably enhance the maturity of mouse embryonic cardiac cells for cardiac function in terms of significant regulation of key genes, such as GATA-4, c-TnT, and Nkx 2.5 with α-MHC, in comparison to the cells onto Nylon alone nanofibers, pointing that the introduction of MoS_2 can cooperatively help cardiac renascence and possibly play a pivotal role in the amplification of myocardium growth and maturation [208].

In a study carried out by wang et al., MoS_2 thin films were synthesized on a glass substrate for neural stem cell culture [209]. The conductivity of the synthesized platform is essential and effective in neural cell differentiation. Also, the porous structure of the platform influences cell behavior. They demonstrated that the platform is biocompatible and cytocompatible and promotes the maturation of neural tissues. Most recent cases of employing MoS_2 for tissue engineering applications are listed in Table 3.

9. Other biomedical applications of structures based on MoS_2

In recent years, MoS_2 nanosheets with large surface area, their interesting physical and chemical properties, and their many applications in various fields have attracted the attention of many researchers [219]. They have multiple applications in the fields of catalysis, lubrication, hydrogen storage, gas sensors, supercapacitors, lithium batteries, optoelectronics, and biomedicine [220,221]. Among the biomedical applications of two-dimensional molybdenum disulfide nanostructures, we can mention drug delivery, phototherapy, and tissue engineering. In addition, there are other emerging biomedical applications, such as biosensors, and bioimaging, which will be briefly explained in this section.

2D-MoS_2 is rapidly becoming a popular material for biosensing applications, and a considerable number of publications on its incorporation into biosensing have emerged in recent years. The high surface area-to-volume ratio and layered structure of this material allow it to accommodate a large amount of chemical/bio species. Two-dimensional MoS_2 exhibits functional versatility, desirable optical and electronic properties, and unique vibrational properties, presenting distinct advantages for establishing biosensors [222,223]. Various types of biosensors have been developed using MoS_2 and its composites, including electrochemical, optical, and FET-based biosensors [224]. Biosensor technology uses bioactive units (such as enzymes, antibodies, nucleic acids, and cells) as an element to detect a wide variety of chemical molecules and biomolecules with high specificity and sensitivity. Cui's group developed an electrochemical biosensor based on multilayered molybdenum disulfide nanosheets for highly sensitive detection of circulating tumor DNA (ctDNA) [225]. The produced MoS_2 nanosheets displayed good electrochemical activity. The bioassay platform was developed based on the differential affinity of MoS_2 nanosheets for single-stranded DNA (ssDNA) and double-stranded DNA (dsDNA). The signal molecule used in this work was methylene blue. The findings demonstrated that this sensor's ability to detect ctDNA has an outstanding linear relationship over various concentrations and a reasonable detection limit. This sensor has excellent characteristics and stability. This technology offers an alternate method for ctDNA detection and a successful assay strategy for upcoming label-free in vitro cancer diagnosis.

Bioimaging uses light, electrons, X-ray, positrons, ultrasound, and magnetic resonance (MR) as imaging sources [226]. MoS_2 QDs have emerged as one of the potential candidates for bioimaging among all the known layered materials. MoS_2 QDs exhibit good single-photon and two-photon fluorescence imaging characteristics, excellent stability in physiological fluids, and good biocompatibility [227]. Roy et al. studied an efficient method for targeted bioimaging of cancer cells using free folic acid-sensitive molybdenum disulfide quantum dots through fluorescence "Turn-Off" [228]. Because of MoS_2 QDs' high selectivity and sensitivity to FA, the MoS_2 QD-based nanoprobe is an ideal candidate for FA-targeted "turn-off" imaging probes for in vivo studies of FA-pretreated FR-overexpressed cancer cells. As a result, these MoS_2 QD-based nanoprobes can be used as potential nanoprobes for cancer prediagnosis via targeted bioimaging.

10. Conclusion and future perspectives

2D MoS_2 nanosheets have been studied exponentially in recent years and have achieved remarkable results in biomedical applications. As a result of research in this field, various excellent properties have been discovered for MoS_2 nanosheets, which are widely used today.

In this study, we reviewed the latest literature on molybdenum disulfide as a subset of transition metal dichalcogenides, which has been explored more than other 2D metal sulfide nanosheets with a unique two-dimensional layered structure. We have studied the various structures of MoS_2 and their synthesis techniques in detail. Different synthesis methods enable researchers to fine-tune the properties for the intended application. Outstanding features, including the high degree of anisotropy, suitable hydrodynamic diameter, mechanical strength,

Table 3
Most recent MoS_2-based platforms for tissue engineering.

Platform	Application	Highlights	Year	Ref.
MoS_2 quantum dots/ gelatin methacryloyl	Tissue engineering	A porous platform as an oxygen carrier and photo-induced oxygen release capability for tissue repair and wound healing	2019	[210]
Polycaprolactone/ zein/MoS_2	Tissue-engineered bone	The biocompatible electrospun nanocomposite shows improved cell attachment and proliferation properties for preosteoblast cell lines	2020	[211]
Poly (lactic-co-glycolic acid)/ borosilicate bioactive glass/ MoS_2	Bone repair	The platform can improve the differentiation and proliferation of rat bone cells. This composite shows photothermal conversion properties and enhanced drug load and release capability	2020	[212]
Silk fibroin/MoS_2	cardiac tissue engineering	The nanofibers of this composite were obtained by electrospinning and showed biocompatibility and significant cell attachment. Also, cardiac genes maturated on the surface of silk fibroin/ MoS_2 scaffolds	2020	[213]
Polyaniline/MoS_2/ polyvinylidene fluoride	Tissue-engineered bone	The scaffold with piezoelectric properties and improved electrical stimulation for the maturation of bone cells	2021	[214]
MoS_2/WS2 nanofilm	Tissue engineering	The nanofilm changes the behavior of the cell under a magnetic field and is helpful in cell culture applications	2021	[215]
Gelatin/MoS_2 hydrogel	Tissue engineering	This biomimetic platform shows excellent self-healing and mechanical properties. It can be used in biomedical applications due to its injectability and processability	2021	[216]
Polycaprolactone/ MoS_2/ decellularized human amniotic membrane	Cardiac tissue regeneration	The cellular matrix and electrical conductivity of the platform are similar to the myocardium	2022	[217]
MoS_2/biotin/ agarose/gelatin	Tissue-engineered bone	A biocompatible platform with osteogenesis induction properties under near IR irradiation	2022	[218]

homogenous morphology, biocompatibility, large surface area, availability of surface modification methods for enhanced functionality, distinctive band gap structure, high absorbance in the near-infrared region, remarkable magnetic attributes, low friction that can be used as a suitable lubricant, and high MoS_2 strength make MoS_2 a promising candidate for diverse applications, particularly for combined therapy due to the large surface area of MoS_2 and high photothermal conversion efficiency, bioimaging, and biosensing as discussed in this article.

Despite the promising features of MoS_2, several impediments must be addressed toward effective use in biomedical applications. Poor stability and dispersibility of MoS_2 in aqueous solutions is a significant challenge limiting its application in biomedical fields. Surface modification of MoS_2 with different biopolymers has been proposed to tackle this challenge. Bovine serum albumin (BSA), polyethylene glycol (PEG), poly (acrylic acid) (PAA), chitosan, and glutathione are among the polymers used to modify the surface of MoS_2 to enhance its stability and prolong its circulation period in the bloodstream. Also, hyperbranched polymers have shown better results in protracting the blood circulation time.

Additionally, despite various functionalization methods being proposed, the functionalization of MoS_2-based nanomaterials is more complicated than that of graphene, which requires more profound investigation. Graphene can be functionalized at the basal plane and the edges, whereas MoS_2 is not highly reactive in the basal plane since chalcogen atoms are saturated, and embedded Mo atoms beneath the chalcogen layer make functionalization harder. Hence, extensive study is required to develop green synthesis approaches and facile surface modification methods for enhanced targeting, stability, and achieving control over size distribution since size distribution plays a pivotal role in nanomaterials toxicity and faster clearance from the bloodstream.

Another challenge in using MoS_2 nanoparticles is developing facile preparation methods that are easy to scale up. The developed methods should consider homogenous morphology, surface modification approach to realize biocompatibility and stability, and high therapeutic efficiency as primary objectives. In this regard, decorating the fabricated MoS_2-based platforms with targeting ligands and conjugating with drugs is a novel and promising approach for further study in the future.

Also, more research is required on the biosafety of MoS_2 nanoparticles by evaluating their in vivo toxicity and studying their long-term effect on the body through tracking MoS_2-based platforms' metabolic pathways to pave the way toward clinical trials.

Integrating diagnosis and treatment is another imperative that can be achieved through a combination of bioimaging and photothermal therapy.

Regarding tissue engineering applications of MoS_2, it is also necessary to have more comprehensive information on the biodegradation behavior and long-term toxicity of the fabricated scaffolds. Moreover, a systematic study is required to improve the physiological stability, metabolic pathways, and biodistribution of the composite scaffolds fabricated by using various biomaterials. Also, further development of synergistic therapy strategies using composite scaffolds is needed.

MoS_2 in developing biosensors requires developing multifunctional nanocomposites and further attention to MoS_2-based devices with more specific bio interactions to achieve ultra-low detection limits to develop ultra-sensitive biosensors and facilitate clinical diagnosis.

To recapitulate, MoS_2 is a potential candidate for nanomedicine with promising attributes and requires extensive research on the remaining challenges. Collaboration among researchers from different disciplines is crucial to overcome the shortcomings and realize the successful clinical translation of MoS_2 as the ultimate goal.

Declaration of competing interest

The authors declare no conflicts of interest.

Data availability

Data will be made available on request.

References

[1] F. Laffleur, V. Keckeis, Advances in drug delivery systems: work in progress still needed? Int. J. Pharm. X. 2 (2020).
[2] S. Adepu, S. Ramakrishna, Controlled drug delivery systems: current status and future directions, Molecules 26 (2021) 5905.
[3] K.K. Jain, Drug delivery systems - an overview, Methods Mol. Biol. 437 (2008) 1–50, https://doi.org/10.1007/978-1-59745-210-6_1/COVER.
[4] C. Li, J. Wang, Y. Wang, H. Gao, G. Wei, Y. Huang, H. Yu, Y. Gan, Y. Wang, L. Mei, Recent progress in drug delivery, Acta Pharm. Sin. B. 9 (2019) 1145–1162.
[5] A. Samadi, F. Yazdian, M. Navaei-Nigjeh, H. Rashedi, Nanocomposite hydrogels: a promising approach for developing stimuli-responsive platforms and their application in targeted drug delivery, J. Shahid Sadoughi Univ. Med. Sci. 29 (2021) 3877–3897, https://doi.org/10.18502/ssu.v29i7.7263.
[6] A. Samadi, S. Haseli, M. Pourmadadi, H. Rashedi, F. Yazdian, M. Navaei-Nigjeh, Curcumin-loaded chitosan-agarose-montmorillonite hydrogel nanocomposite for the treatment of breast cancer, in: 27th Natl. 5th Int. Iran. Conf. Biomed. Eng. ICBME 2020, 2020, pp. 148–153, https://doi.org/10.1109/ICBME51989.2020.9319425.
[7] M. Ahmadi, M. Pourmadadi, S.A. Ghorbanian, F. Yazdian, H. Rashedi, Ultra pH-sensitive nanocarrier based on Fe2O3/chitosan/montmorillonite for quercetin delivery, Int. J. Biol. Macromol. 191 (2021) 738–745, https://doi.org/10.1016/J.IJBIOMAC.2021.09.023.
[8] H. Lu, J. Wang, T. Wang, J. Zhong, Y. Bao, H. Hao, Recent progress on nanostructures for drug delivery applications, J. Nanomater. 2016 (2016).
[9] R.G. Mendes, A. Bachmatiuk, B. Büchner, G. Cuniberti, M.H. Rümmeli, Carbon nanostructures as multi-functional drug delivery platforms, J. Mater. Chem. B. 1 (2013) 401–428.
[10] M. Razavi, J. Wang, A.S. Thakor, Localized drug delivery graphene bioscaffolds for cotransplantation of islets and mesenchymal stem cells, Sci. Adv. 7 (2021), eabf9221.
[11] N. Işıklan, N.A. Hussien, M. Türk, Synthesis and drug delivery performance of gelatin-decorated magnetic graphene oxide nanoplatform, Colloids Surfaces A Physicochem. Eng. Asp. 616 (2021), 126256.
[12] M. Zamani, M. Pourmadadi, S.A. Seyyed Ebrahimi, F. Yazdian, J. Shabani Shayeh, A novel labeled and label-free dual electrochemical detection of endotoxin based on aptamer-conjugated magnetic reduced graphene oxide-gold nanocomposite, J. Electroanal. Chem. 908 (2022), 116116, https://doi.org/10.1016/J.JELECHEM.2022.116116.
[13] A.S. Ghasemi, B. Makiabadi, M. Zakarianezhad, A. Soltani, F. Ashrafi, F. Mashhadban, Experimental and theoretical studies of the interaction of Penicillamine with SWCNT (6, 0) as a drug delivery system, Inorg. Nano-Metal Chem (2022) 1–9.
[14] M. Rahamathulla, R.R. Bhosale, R.A.M. Osmani, K.C. Mahima, A.P. Johnson, U. Hani, M. Ghazwani, M.Y. Begum, S. Alshehri, M.M. Ghoneim, Carbon nanotubes: current perspectives on diverse applications in targeted drug delivery and therapies, Materials 14 (2021) 6707.
[15] H. Kazemzadeh, M. Mozafari, Fullerene-based delivery systems, Drug Discov. Today 24 (2019) 898–905.
[16] J. Dong, Y. Zhao, K. Wang, H. Chen, L. Liu, B. Sun, M. Yang, L. Sun, Y. Wang, X. Yu, Fabrication of graphitic carbon nitride quantum dots and their application for simultaneous fluorescence imaging and pH-responsive drug release, ChemistrySelect 3 (2018) 12696–12703.
[17] S. Anju, P.V. Mohanan, Biomedical applications of transition metal dichalcogenides (TMDCs), Synth. Met. 271 (2021), 116610.
[18] M. Emanet, Ö. Şen, M. Çulha, Evaluation of boron nitride nanotubes and hexagonal boron nitrides as nanocarriers for cancer drugs, Nanomedicine 12 (2017) 797–810.
[19] A. Sharma, A.K. Goyal, G. Rath, Recent advances in metal nanoparticles in cancer therapy, J. Drug Target. 26 (2018) 617–632.
[20] K.R.B. Singh, V. Nayak, J. Singh, A.K. Singh, R.P. Singh, Potentialities of bioinspired metal and metal oxide nanoparticles in biomedical sciences, RSC Adv. 11 (2021) 24722–24746.
[21] H. Sharma, K. Kumar, C. Choudhary, P.K. Mishra, B. Vaidya, Development and characterization of metal oxide nanoparticles for the delivery of anticancer drug, Artif. Cells, Nanomedicine, Biotechnol. 44 (2016) 672–679.
[22] M. Fizir, P. Dramou, N.S. Dahiru, W. Ruya, T. Huang, H. He, Halloysite nanotubes in analytical sciences and in drug delivery: a review, Microchim. Acta 185 (2018) 1–33.
[23] R. Bilan, I. Nabiev, A. Sukhanova, Quantum dot-based nanotools for bioimaging, diagnostics, and drug delivery, ChemBioChem 17 (2016) 2103–2114.
[24] H.S. Han, K.Y. Choi, Advances in nanomaterial-mediated photothermal cancer therapies: toward clinical applications, Biomedicines 9 (2021) 305.
[25] C. Caro, F. Gámez, P. Quaresma, J.M. Páez-Muñoz, A. Domínguez, J.R. Pearson, M. Pernía Leal, A.M. Beltrán, Y. Fernandez-Afonso, J.M. De la Fuente, Fe3O4-Au core-shell nanoparticles as a multimodal platform for in vivo imaging and focused photothermal therapy, Pharmaceutics 13 (2021) 416.
[26] H. Zhu, Z. Li, E. Ye, D.T. Leong, Oxygenic enrichment in hybrid Ruthenium sulfide nanoclusters for an optimized photothermal effect, ACS Appl. Mater. Interfaces 13 (2021) 60351–60361.
[27] P. McKernan, N.A. Virani, G.N.F. Faria, C.G. Karch, R.P. Silvy, D.E. Resasco, L. F. Thompson, R.G. Harrison, Targeted single-walled carbon nanotubes for photothermal therapy combined with immune checkpoint inhibition for the treatment of metastatic breast cancer, Nanoscale Res. Lett. 16 (2021) 1–9.
[28] M. Gao, H. Zhao, Z. Wang, Y. Zhao, X. Zou, L. Sun, Controllable preparation of Ag2S quantum dots with size-dependent fluorescence and cancer photothermal therapy, Adv. Powder Technol. 32 (2021) 1972–1982.
[29] C. Yin, X. Li, Y. Wang, Y. Liang, S. Zhou, P. Zhao, C. Lee, Q. Fan, W. Huang, Organic semiconducting macromolecular dyes for NIR-II photoacoustic imaging and photothermal therapy, Adv. Funct. Mater. 31 (2021), 2104650.
[30] Y. Zhang, X. He, Y. Zhang, Y. Zhao, S. Lu, Y. Peng, L. Lu, X. Hu, M. Zhan, Native mitochondria-targeting polymeric nanoparticles for mild photothermal therapy rationally potentiated with immune checkpoints blockade to inhibit tumor recurrence and metastasis, Chem. Eng. J. 424 (2021), 130171.
[31] M. Liu, H. Zhu, Y. Wang, C. Sevencan, B.L. Li, Functionalized mos2-based nanomaterials for cancer phototherapy and other biomedical applications, ACS Mater. Lett. 3 (2021) 462–496.
[32] S. Chee, W. Lee, Y. Jo, M.K. Cho, D. Chun, H. Baik, B. Kim, M. Yoon, K. Lee, M. Ham, Atomic vacancy control and elemental substitution in a monolayer molybdenum disulfide for high performance optoelectronic device arrays, Adv. Funct. Mater. 30 (2020), 1908147.
[33] M. Chhowalla, H.S. Shin, G. Eda, L.-J. Li, K.P. Loh, H. Zhang, The chemistry of two-dimensional layered transition metal dichalcogenide nanosheets, Nat. Chem. 5 (2013) 263–275.
[34] G. Eda, H. Yamaguchi, D. Voiry, T. Fujita, M. Chen, M. Chhowalla, Photoluminescence from chemically exfoliated MoS2, Nano Lett. 11 (2011) 5111–5116.
[35] C.V. Ramana, U. Becker, V. Shutthanandan, C.M. Julien, Oxidation and metal-insertion in molybdenite surfaces: evaluation of charge-transfer mechanisms and dynamics, Geochem. Trans. 9 (2008) 1–8.
[36] D. Saha, P. Kruse, Editors' choice—review—conductive forms of MoS2 and their applications in energy storage and conversion, J. Electrochem. Soc. 167 (2020), 126517.
[37] X. Li, H. Zhu, Two-dimensional MoS2: properties, preparation, and applications, J. Mater. 1 (2015) 33–44.
[38] G. Tang, Y. Chen, J. Yin, S. Shen, K. Cai, Preparation, characterization and properties of MoS2 nanosheets via a microwave-assisted wet-chemical route, Ceram. Int. 44 (2018) 5336–5340.
[39] D. Gupta, V. Chauhan, R. Kumar, A comprehensive review on synthesis and applications of molybdenum disulfide (MoS2) material: past and recent developments, Inorg. Chem. Commun. 121 (2020), 108200.
[40] S. Alam, M.A. Chowdhury, A. Shahid, R. Alam, A. Rahim, Synthesis of emerging two-dimensional (2D) materials–Advances, challenges and prospects, FlatChem 30 (2021), 100305.
[41] X. Zhang, S.Y. Teng, A.C.M. Loy, B.S. How, W.D. Leong, X. Tao, Transition metal dichalcogenides for the application of pollution reduction: a review, Nanomaterials 10 (2020) 1012.
[42] J. Wei, W. Li, B. Liao, B. Bian, Electronic and optical properties of vertical borophene/MoS2 heterojunctions, Mater. Chem. Phys. 252 (2020), 123305.
[43] H. Xu, M.K. Akbari, S. Zhuiykov, 2D Semiconductor nanomaterials and heterostructures: controlled synthesis and functional applications, Nanoscale Res. Lett. 16 (2021) 1–38.
[44] W. Choi, N. Choudhary, G.H. Han, J. Park, D. Akinwande, Y.H. Lee, Recent development of two-dimensional transition metal dichalcogenides and their applications, Mater, Today Off. 20 (2017) 116–130.
[45] A. Sebastian, R. Pendurthi, T.H. Choudhury, J.M. Redwing, S. Das, Benchmarking monolayer MoS2 and WS2 field-effect transistors, Nat. Commun. 12 (2021) 1–12.
[46] A. Splendiani, L. Sun, Y. Zhang, T. Li, J. Kim, C.-Y. Chim, G. Galli, F. Wang, Emerging photoluminescence in monolayer MoS2, Nano Lett. 10 (2010) 1271–1275.
[47] G. Zhang, H. Liu, J. Qu, J. Li, Two-dimensional layered MoS 2: rational design, properties and electrochemical applications, Energy Environ. Sci. 9 (2016) 1190–1209.
[48] I.N. Yakovkin, Dirac cones in graphene, interlayer interaction in layered materials, and the band gap in MoS2, Crystals 6 (2016) 143.
[49] J.K. Ellis, M.J. Lucero, G.E. Scuseria, The indirect to direct band gap transition in multilayered MoS2 as predicted by screened hybrid density functional theory, Appl. Phys. Lett. 99 (2011), 261908.
[50] K.F. Mak, C. Lee, J. Hone, J. Shan, T.F. Heinz, Atomically thin MoS 2: a new direct-gap semiconductor, Phys. Rev. Lett. 105 (2010), 136805.
[51] S. Sarma, S.C. Ray, Magnetic behaviors of single crystal-MoS2 (MoS2-SC) and nanoparticle-MoS2 (MoS2-NP) and bi-layer-MoS2 thin film, J. Magn. Magn Mater. 546 (2022), 168863.
[52] M.G. Choi, A. Belianinov, A. Pawlicki, S. Park, H. Lee, O.S. Ovchinnikova, S. Kim, Nanoscale friction of CVD single-layer MoS2 with controlled defect formation, Surface. Interfac. 26 (2021), 101437.
[53] K.K. Singh, R. Prabhu, B, S. Choudhary, C. Pramanik, N.S. John, Effect of graphene and MoS2 flakes in industrial oils to enhance lubrication, ACS Omega 4 (2019) 14569–14578.
[54] W.O. Winer, Molybdenum disulfide as a lubricant: a review of the fundamental knowledge, Wear 10 (1967) 422–452.

[55] S.B. Mousavi, S.Z. Heris, P. Estellé, Experimental comparison between ZnO and MoS2 nanoparticles as additives on performance of diesel oil-based nano lubricant, Sci. Rep. 10 (2020) 1–17.
[56] P.-R. Wu, Z. Liu, Z.-L. Cheng, Growth of MoS2 nanotubes templated by halloysite nanotubes for the reduction of friction in oil, ACS Omega 3 (2018) 15002–15008.
[57] V. Kotsyubynsky, L. Shyyko, T. Shihab, P. Prysyazhnyuk, V. Aulin, V. Boichuk, Multilayered MoS2/C nanospheres as high performance additives to lubricating oils, Mater. Today Proc. 35 (2021) 538–541.
[58] E. Serpini, A. Rota, S. Valeri, E. Ukraintsev, B. Rezek, T. Polcar, P. Nicolini, Nanoscale frictional properties of ordered and disordered MoS2, Tribol. Int. 136 (2019) 67–74.
[59] R.K. Zahedi, N. Alajlan, H.K. Zahedi, T. Rabczuk, Mechanical properties of all MoS2 monolayer heterostructures: crack propagation and existing notch study, Comput. Mater. Continua (CMC) 70 (2022) 4635–4655.
[60] M.J. Akhter, W. Kuś, A. Mrozek, T. Burczyński, Mechanical properties of monolayer MoS2 with randomly distributed defects, Materials 13 (2020) 1307.
[61] J. Jian, H. Chang, T. Xu, Structure and properties of single-layer MoS2 for nano-photoelectric devices, Materials 12 (2019) 198.
[62] N. Baig, I. Kammakakam, W. Falath, Nanomaterials: a review of synthesis methods, properties, recent progress, and challenges, Mater. Adv 2 (2021) 1821–1871.
[63] P. Khanna, A. Kaur, D. Goyal, Algae-based metallic nanoparticles: synthesis, characterization and applications, J. Microbiol. Methods 163 (2019), 105656.
[64] S. Kumar, P. Bhushan, S. Bhattacharya, Fabrication of nanostructures with bottom-up approach and their utility in diagnostics, therapeutics, and others, in: Environ. Chem. Med. Sensors, Springer, 2018, pp. 167–198.
[65] K.S. Novoselov, D. Jiang, F. Schedin, T.J. Booth, V.V. Khotkevich, S.V. Morozov, A.K. Geim, Two-dimensional atomic crystals, Proc. Natl. Acad. Sci. USA 102 (2005) 10451–10453.
[66] R.S. Sharbidre, S.M. Park, C.J. Lee, B.C. Park, S.-G. Hong, S. Bramhe, G.Y. Yun, J.-K. Ryu, T.N. Kim, Reliable and high spatial Resolution method to identify the number of MoS 2 layers using a scanning electron microscopy, Korean J. Mater. Res. 27 (2017) 705–709.
[67] W. Li, Y. Zhang, X. Long, J. Cao, X. Xin, X. Guan, J. Peng, X. Zheng, Gas sensors based on mechanically exfoliated MoS2 nanosheets for room-temperature NO2 detection, Sensors 19 (2019) 2123.
[68] S. Kaushik, U.K. Tiwari, R.K. Choubey, K. Singh, R.K. Sinha, Study of sonication assisted synthesis of molybdenum disulfide (MoS2) nanosheets, Mater, Today Proc 21 (2020) 1969–1975.
[69] Y. Huang, C. Wan, Controllable fabrication and multifunctional applications of graphene/ceramic composites, J. Adv. Ceram. 9 (2020) 271–291.
[70] F.I. Alzakia, S.C. Tan, Liquid-exfoliated 2D materials for optoelectronic applications, Adv. Sci. 8 (2021), 2003864.
[71] D. Sahoo, B. Kumar, J. Sinha, S. Ghosh, S.S. Roy, B. Kaviraj, Cost effective liquid phase exfoliation of MoS2 nanosheets and photocatalytic activity for wastewater treatment enforced by visible light, Sci. Rep. 10 (2020) 1–12.
[72] A. Winchester, S. Ghosh, S. Feng, A.L. Elias, T. Mallouk, M. Terrones, S. Talapatra, Electrochemical characterization of liquid phase exfoliated two-dimensional layers of molybdenum disulfide, ACS Appl. Mater. Interfaces 6 (2014) 2125–2130.
[73] J.R. Brent, N. Savjani, P. O'Brien, Synthetic approaches to two-dimensional transition metal dichalcogenide nanosheets, Prog. Mater. Sci. 89 (2017) 411–478.
[74] Y.D. Liu, L. Ren, X. Qi, L.W. Yang, G.L. Hao, J. Li, X.L. Wei, J.X. Zhong, Preparation, characterization and photoelectrochemical property of ultrathin MoS2 nanosheets via hydrothermal intercalation and exfoliation route, J. Alloys Compd. 571 (2013) 37–42.
[75] C.A. Salagean, C. Costinas, L.C. Cotet, L. Baia, Insights into the influence of key preparation parameters on the performance of MoS2/graphene oxide composites as active materials in supercapacitors, Catalysts 11 (2021) 1553.
[76] L. Ndlwana, N. Raleie, K.M. Dimpe, H.F. Ogutu, E.O. Oseghe, M.M. Motsa, T.A. M. Msagati, B.B. Mamba, Sustainable hydrothermal and solvothermal synthesis of advanced carbon materials in multidimensional applications: a review, Materials 14 (2021) 5094.
[77] K. Hou, S. Liu, G. Liao, H. Qiao, J. Li, X. Qi, Simple hydrothermal synthesis of molybdenum disulfide and its application for a large-area photodetector, Cryst. Res. Technol. 55 (2020), 2000053.
[78] C.M. Lee, G.C. Park, S.M. Lee, J.H. Choi, S.H. Jeong, T.Y. Seo, S.-B. Jung, J. H. Lim, J. Joo, Effects of precursor concentration on morphology of MoS2 Nanosheets by hydrothermal synthesis, J. Nanosci. Nanotechnol. 16 (2016) 11548–11551.
[79] J. Dong, L. Zhang, B. Wu, F. Ding, Y. Liu, Theoretical study of chemical vapor deposition synthesis of graphene and beyond: challenges and perspectives, J. Phys. Chem. Lett. 12 (2021) 7942–7963.
[80] J. Zhang, T. Liu, L. Fu, G. Ye, Synthesis of nanosized ultrathin MoS2 on montmorillonite nanosheets by CVD method, Chem. Phys. Lett. 781 (2021), 138972.
[81] J. Jeon, S.K. Jang, S.M. Jeon, G. Yoo, Y.H. Jang, J.-H. Park, S. Lee, Layer-controlled CVD growth of large-area two-dimensional MoS 2 films, Nanoscale 7 (2015) 1688–1695.
[82] Y. Yang, H. Pu, T. Lin, L. Li, S. Zhang, G. Sun, Growth of monolayer MoS2 films in a quasi-closed crucible encapsulated substrates by chemical vapor deposition, Chem. Phys. Lett. 679 (2017) 181–184.
[83] E. Benavente, M.A. Santa Ana, F. Mendizábal, G. González, Intercalation chemistry of molybdenum disulfide, Coord. Chem. Rev. 224 (2002) 87–109, https://doi.org/10.1016/S0010-8545(01)00392-7.
[84] Y. Wu, J. Wang, Y. Li, J. Zhou, B.Y. Wang, A. Yang, L.-W. Wang, H.Y. Hwang, Y. Cui, Observation of an intermediate state during lithium intercalation of twisted bilayer MoS2, Nat. Commun. 2022 131 (2022) 1–8, https://doi.org/10.1038/s41467-022-30516-z, 13.
[85] A. Ambrosi, Z. Sofer, M. Pumera, Lithium intercalation compound dramatically influences the electrochemical properties of exfoliated MoS2, Small 11 (2015) 605–612, https://doi.org/10.1002/smll.201400401.
[86] A. Ejigu, I.A. Kinloch, E. Prestat, R.A.W. Dryfe, A simple electrochemical route to metallic phase trilayer MoS2: evaluation as electrocatalysts and supercapacitors, J. Mater. Chem. A. 5 (2017) 11316–11330, https://doi.org/10.1039/c7ta02577g.
[87] G.H. Lee, J.W. Jeong, S.H. Huh, S.H. Kim, B.J. Choi, Y.W. Kim, A Simple Synthetic Route to MoS2 and WS2 Nanoparticles and Thin Films 17 (2012) 1134–1140, https://doi.org/10.1142/S0217979203018636. Https://Doi.Org/10.1142/S0217979203018636.
[88] S. Thangudu, M.T. Lee, S. Rtimi, Tandem synthesis of high yield mos2 nanosheets and enzyme peroxidase mimicking properties, Catalysts 10 (2020) 1–11, https://doi.org/10.3390/catal10091009.
[89] C. Feng, J. Ma, H. Li, R. Zeng, Z. Guo, H. Liu, Synthesis of molybdenum disulfide (MoS2) for lithium ion battery applications, Mater. Res. Bull. 44 (2009) 1811–1815, https://doi.org/10.1016/j.materresbull.2009.05.018.
[90] K.-G. Zhou, N.-N. Mao, H.-X. Wang, Y. Peng, H.-L. Zhang, K.-G. Zhou, N.-N. Mao, H.-X.H. Wang, -L. Zhang, Y. Peng, A mixed-solvent strategy for efficient exfoliation of inorganic graphene analogues, Angew. Chem. Int. Ed. 50 (2011) 10839–10842, https://doi.org/10.1002/ANIE.201105364.
[91] M. Yi, C. Zhang, The synthesis of two-dimensional MoS 2 nanosheets with enhanced tribological properties as oil additives, RSC Adv. 8 (2018) 9564–9573.
[92] G. Solomon, R. Mazzaro, V. Morandi, I. Concina, A. Vomiero, Microwave-assisted vs. conventional hydrothermal synthesis of MoS2 nanosheets: application towards hydrogen evolution reaction, Crystals 10 (2020) 1040.
[93] S. Kim, W. Park, D. Kim, J. Kang, J. Lee, H.Y. Jang, S.H. Song, B. Cho, D. Lee, Novel exfoliation of high-quality 2h-mos2 nanoflakes for solution-processed photodetector, Nanomaterials 10 (2020) 1045.
[94] H. Kim, T. Park, M. Leem, H. Lee, W. Ahn, E. Lee, H. Kim, Sulfidation characteristics of amorphous nonstoichiometric Mo-oxides for MoS2 synthesis, Appl. Surf. Sci. 535 (2021), 147684.
[95] P. Wang, X. Wang, F. Tan, R. Zhang, Residual oxygen effects on the properties of MoS2 thin films deposited at different temperatures by magnetron sputtering, Crystals 11 (2021) 1183.
[96] I.V. Tudose, F. Comanescu, P. Pascariu, S. Bucur, L. Rusen, F. Iacomi, E. Koudoumas, M.P. Suchea, Chemical and Physical Methods for Multifunctional Nanostructured Interface Fabrication, Elsevier Inc., 2019, https://doi.org/10.1016/B978-0-12-814401-5.00002-5.
[97] A. Stergiou, N. Tagmatarchis, Molecular functionalization of two-dimensional MoS2 nanosheets, Chem. Eur J. 24 (2018) 18246–18257.
[98] S. Presolski, M. Pumera, Covalent functionalization of MoS2, mater, Today Off. 19 (2016) 140–145.
[99] I.K. Sideri, R. Arenal, N. Tagmatarchis, Covalently functionalized MoS2 with dithiolenes, ACS Mater. Lett. 2 (2020) 832–837.
[100] W.S. Seo, D.K. Kim, J.-H. Han, K.-B. Park, S.C. Ryu, N.K. Min, J.H. Kim, Functionalization of molybdenum disulfide via plasma treatment and 3-mercaptopropionic acid for gas sensors, Nanomaterials 10 (2020) 1860.
[101] S. Xu, Y. Zhong, C. Nie, Y. Pan, M. Adeli, R. Haag, Co-Delivery of doxorubicin and chloroquine by polyglycerol functionalized MoS2 nanosheets for efficient multidrug-resistant cancer therapy, Macromol. Biosci. 21 (2021), 2100233.
[102] H. Liu, D. Grasseschi, A. Dodda, K. Fujisawa, D. Olson, E. Kahn, F. Zhang, T. Zhang, Y. Lei, R.B.N. Branco, Spontaneous chemical functionalization via coordination of Au single atoms on monolayer MoS2, Sci. Adv. 6 (2020), eabc9308.
[103] J. Zheng, K. Lebedev, S. Wu, C. Huang, T. Ayvalı, T.-S. Wu, Y. Li, P.-L. Ho, Y.-L. Soo, A. Kirkland, High loading of transition metal single atoms on chalcogenide catalysts, J. Am. Chem. Soc. (2021).
[104] L. Daukiya, J. Teyssandier, S. Eyley, S. El Kazzi, M.C.R. González, B. Pradhan, W. Thielemans, J. Hofkens, S. De Feyter, Covalent functionalization of molybdenum disulfide by chemically activated diazonium salts, Nanoscale 13 (2021) 2972–2981.
[105] M. Vera-Hidalgo, E. Giovanelli, C. Navio, E.M. Perez, Mild covalent functionalization of transition metal dichalcogenides with maleimides: a "click" reaction for 2H-MoS2 and WS2, J. Am. Chem. Soc. 141 (2019) 3767–3771.
[106] S. García-Dalí, J.I. Paredes, S. Villar-Rodil, A. Martínez-Jódar, A. Martínez-Alonso, J.M.D. Tascon, Molecular functionalization of 2H-phase MoS2 nanosheets via an electrolytic route for enhanced catalytic performance, ACS Appl. Mater. Interfaces 13 (2021) 33157–33171.
[107] P.K. Mohapatra, K. Ranganathan, L. Dezanashvili, L. Houben, A. Ismach, Epitaxial growth of In2Se3 on monolayer transition metal dichalcogenide single crystals for high performance photodetectors, Appl. Mater. Today 20 (2020), 100734.
[108] M. Xie, N. Yang, J. Cheng, M. Yang, T. Deng, Y. Li, C. Feng, Layered MoS2 nanosheets modified by biomimetic phospholipids: enhanced stability and its synergistic treatment of cancer with chemo-photothermal therapy, Colloids Surf. B Biointerfaces 187 (2020), 110631.
[109] K. Zhang, Y. Zhuang, W. Zhang, Y. Guo, X. Liu, Functionalized MoS2-nanoparticles for transdermal drug delivery of atenolol, Drug Deliv. 27 (2020) 909–916.
[110] M.C. Scicluna, L. Vella-Zarb, Evolution of nanocarrier drug-delivery systems and recent advancements in covalent organic framework–drug systems, ACS Appl. Nano Mater. 3 (2020) 3097–3115.

[111] F.M. Veronese, A. Mero, The impact of PEGylation on biological therapies, BioDrugs 22 (2008) 315–329.
[112] T. Liu, S. Shi, C. Liang, S. Shen, L. Cheng, C. Wang, X. Song, S. Goel, T.E. Barnhart, W. Cai, Iron oxide decorated MoS2 nanosheets with double PEGylation for chelator-free radiolabeling and multimodal imaging guided photothermal therapy, ACS Nano 9 (2015) 950–960.
[113] T.R.S. Malagrino, A.P. Godoy, J.M. Barbosa, A.G.T. Lima, N.C.O. Sousa, J. J. Pedrotti, P.S. Garcia, R.M. Paniago, L.M. Andrade, S.H. Domingues, Multifunctional hybrid MoS2-PEGylated/Au nanostructures with potential theranostic applications in biomedicine, Nanomaterials 12 (2022) 2053.
[114] X. Zhang, J. Wu, G.R. Williams, S. Niu, Q. Qian, L.-M. Zhu, Functionalized MoS2-nanosheets for targeted drug delivery and chemo-photothermal therapy, Colloids Surf. B Biointerfaces 173 (2019) 101–108.
[115] C. Mo, Z. Wang, J. Yang, Y. Ouyang, Q. Mo, S. Li, P. He, L. Chen, X. Li, Rational assembly of RGD/MoS2/Doxorubicin nanodrug for targeted drug delivery, GSH-stimulus release and chemo-photothermal synergistic antitumor activity, J. Photochem. Photobiol. B Biol. (2022), 112487.
[116] A. Sukhanova, S. Bozrova, P. Sokolov, M. Berestovoy, A. Karaulov, I. Nabiev, Dependence of nanoparticle toxicity on their physical and chemical properties, Nanoscale Res. Lett. 13 (2018) 1–21.
[117] Y.-W. Huang, M. Cambre, H.-J. Lee, The toxicity of nanoparticles depends on multiple molecular and physicochemical mechanisms, Int. J. Mol. Sci. 18 (2017) 2702.
[118] H. Bahadar, F. Maqbool, K. Niaz, M. Abdollahi, Toxicity of nanoparticles and an overview of current experimental models, Iran, Biomed. J. 20 (2016) 1.
[119] S. Wilhelm, A.J. Tavares, Q. Dai, S. Ohta, J. Audet, H.F. Dvorak, W.C.W. Chan, Analysis of nanoparticle delivery to tumours, Nat. Rev. Mater. 1 (2016) 1–12.
[120] E. Varrla, C. Backes, K.R. Paton, A. Harvey, Z. Gholamvand, J. McCauley, J. N. Coleman, Large-scale production of size-controlled MoS2 nanosheets by shear exfoliation, Chem. Mater. 27 (2015) 1129–1139.
[121] L. Liu, H. Jiang, J. Dong, W. Zhang, G. Dang, M. Yang, Y. Li, H. Chen, H. Ji, L. Dong, PEGylated MoS2 quantum dots for traceable and pH-responsive chemotherapeutic drug delivery, Colloids Surf. B Biointerfaces 185 (2020), 110590.
[122] X. Dong, W. Yin, X. Zhang, S. Zhu, X. He, J. Yu, J. Xie, Z. Guo, L. Yan, X. Liu, Intelligent MoS2 nanotheranostic for targeted and enzyme-/pH-/NIR-responsive drug delivery to overcome cancer chemotherapy resistance guided by PET imaging, ACS Appl. Mater. Interfaces 10 (2018) 4271–4284.
[123] P. Shah, T.N. Narayanan, C.-Z. Li, S. Alwarappan, Probing the biocompatibility of MoS2 nanosheets by cytotoxicity assay and electrical impedance spectroscopy, Nanotechnology 26 (2015), 315102.
[124] E. Hondroulis, C. Liu, C.-Z. Li, Whole cell based electrical impedance sensing approach for a rapid nanotoxicity assay, Nanotechnology 21 (2010), 315103.
[125] Z. Sobańska, L. Zapor, M. Szparaga, M. Stępnik, Biological effects of molybdenum compounds in nanosized forms under in vitro and in vivo conditions, Int. J. Occup. Med. Environ. Health 33 (2020).
[126] F. Yin, T. Anderson, N. Panwar, K. Zhang, S.C. Tjin, B.K. Ng, H.S. Yoon, J. Qu, K.-T. Yong, Functionalized MoS2 nanosheets as multi-gene delivery vehicles for in vivo pancreatic cancer therapy, Nanotheranostics 2 (2018) 371.
[127] E. Nematollahi, M. Pourmadadi, F. Yazdian, H. Fatoorehchi, H. Rashedi, M. N. Nigjeh, Synthesis and characterization of chitosan/polyvinylpyrrolidone coated nanoporous γ-Alumina as a pH-sensitive carrier for controlled release of quercetin, Int. J. Biol. Macromol. 183 (2021) 600–613, https://doi.org/10.1016/j.ijbiomac.2021.04.160.
[128] S.E. Gerami, M. Pourmadadi, H. Fatoorehchi, F. Yazdian, H. Rashedi, M. N. Nigjeh, Preparation of pH-sensitive chitosan/polyvinylpyrrolidone/α-Fe2O3 nanocomposite for drug delivery application: emphasis on ameliorating restrictions, Int. J. Biol. Macromol. 173 (2021) 409–420, https://doi.org/10.1016/j.ijbiomac.2021.01.067.
[129] S. Haseli, M. Pourmadadi, A. Samadi, F. Yazdian, M. Abdouss, H. Rashedi, M. Navaei-Nigjeh, A novel pH-responsive nanoniosomal emulsion for sustained release of curcumin from a chitosan-based nanocarrier: emphasis on the concurrent improvement of loading, sustained release, and apoptosis induction, Biotechnol. Prog. (2022), https://doi.org/10.1002/BTPR.3280.
[130] M. Danaei, A. Haghdoost, M. Momeni, An epidemiological review of common cancers in Iran, A Review Article TT -, IJBC 11 (2019) 77–84.
[131] M. Yazdani, O. Tavakoli, M. Khoobi, Y.S. Wu, M.A. Faramarzi, E. Gholibegloo, S. Farkhondeh, Beta-carotene/cyclodextrin-based inclusion complex: improved loading, solubility, stability, and cytotoxicity, J. Inclusion Phenom. Macrocycl. Chem. 102 (2022) 55–64, https://doi.org/10.1007/s10847-021-01100-7.
[132] L. Ying, M. Yazdani, R. Koya, R. Zhao, Engineering tumor stromal mechanics for improved T cell therapy, Biochim. Biophys. Acta - Gen. Subj. 1866 (2022), 130095, https://doi.org/10.1016/J.BBAGEN.2022.130095.
[133] M. Pourmadadi, M. Ahmadi, M. Abdouss, F. Yazdian, H. Rashedi, Y. Hesari, The synthesis and characterization of double nanoemulsion for targeted Co-Delivery of 5-fluorouracil and curcumin using pH-sensitive agarose/chitosan nanocarrier, J. Drug Deliv. Sci. Technol. (2021), 102849, https://doi.org/10.1016/j.jddst.2021.102849.
[134] L. Gong, L. Yan, R. Zhou, J. Xie, W. Wu, Z. Gu, Two-dimensional transition metal dichalcogenide nanomaterials for combination cancer therapy, J. Mater. Chem. B. 5 (2017) 1873–1895.
[135] M. Samadi, N. Sarikhani, M. Zirak, H. Zhang, H.L. Zhang, A.Z. Moshfegh, Group 6 transition metal dichalcogenide nanomaterials: synthesis, applications and future perspectives, Nanoscale Horizons 3 (2018) 90–204, https://doi.org/10.1039/c7nh00137a.
[136] H. Kim, S. Beack, S. Han, M. Shin, T. Lee, Y. Park, K.S. Kim, A.K. Yetisen, S. H. Yun, W. Kwon, Multifunctional photonic nanomaterials for diagnostic, therapeutic, and theranostic applications, Adv. Mater. 30 (2018), 1701460.
[137] A. Vadivelmurugan, R. Anbazhagan, V. Arunagiri, J.Y. Lai, H.C. Tsai, Pluronic F127 self-assembled MoS2 nanocomposites as an effective glutathione responsive anticancer drug delivery system, RSC Adv. 9 (2019) 25592–25601, https://doi.org/10.1039/c9ra04249k.
[138] X. Zhu, X. Ji, N. Kong, Y. Chen, M. Mahmoudi, X. Xu, L. Ding, W. Tao, T. Cai, Y. Li, Intracellular mechanistic understanding of 2D MoS2 nanosheets for anti-exocytosis-enhanced synergistic cancer therapy, ACS Nano 12 (2018) 2922–2938.
[139] H.A. Azim Jr., E. De Azambuja, M. Colozza, J. Bines, M.J. Piccart, Long-term toxic effects of adjuvant chemotherapy in breast cancer, Ann. Oncol. 22 (2011) 1939–1947.
[140] C.-L. Tsai, J.-C. Chen, W.-J. Wang, Near-infrared absorption property of biological soft tissue constituents, J. Med. Biol. Eng. 21 (2001) 7–14.
[141] N. Fernandes, C.F. Rodrigues, A.F. Moreira, I.J. Correia, Overview of the application of inorganic nanomaterials in cancer photothermal therapy, Biomater. Sci. 8 (2020) 2990–3020.
[142] S. Liu, X. Pan, H. Liu, Two-dimensional nanomaterials for photothermal therapy, Angew. Chem. 132 (2020) 5943–5953.
[143] T. Liu, C. Wang, W. Cui, H. Gong, C. Liang, X. Shi, Z. Li, B. Sun, Z. Liu, Combined photothermal and photodynamic therapy delivered by PEGylated MoS 2 nanosheets, Nanoscale 6 (2014) 11219–11225.
[144] Q.H. Wang, K. Kalantar-Zadeh, A. Kis, J.N. Coleman, M.S. Strano, Electronics and optoelectronics of two-dimensional transition metal dichalcogenides, Nat. Nanotechnol. 7 (2012) 699–712.
[145] S. Liu, Y. Wang, Facile synthesis of porous MoS2 nanofibers for efficient drug delivery and cancer treatment, Nanotechnology 32 (2021), 385701.
[146] W. Zhang, Z. Guo, D. Huang, Z. Liu, X. Guo, H. Zhong, Synergistic effect of chemo-photothermal therapy using PEGylated graphene oxide, Biomaterials 32 (2011) 8555–8561.
[147] L. Cheng, J. Liu, X. Gu, H. Gong, X. Shi, T. Liu, C. Wang, X. Wang, G. Liu, H. Xing, PEGylated WS2 nanosheets as a multifunctional theranostic agent for in vivo dual-modal CT/photoacoustic imaging guided photothermal therapy, Adv. Mater. 26 (2014) 1886–1893.
[148] J. Zhao, C. Zhou, M. Li, J. Li, G. Li, D. Ma, Z. Li, D. Zou, Bottom-up synthesis of ultra-small molybdenum disulfide-polyvinylpyrrolidone nanosheets for imaging-guided tumor regression, Oncotarget 8 (2017), 106707.
[149] A. Samadi, M. Pourmadadi, F. Yazdian, H. Rashedi, M. Navaei-Nigjeh, T. Eufrasio-da-silva, Ameliorating quercetin constraints in cancer therapy with pH-responsive agarose-polyvinylpyrrolidone -hydroxyapatite nanocomposite encapsulated in double nanoemulsion, Int. J. Biol. Macromol. (2021), https://doi.org/10.1016/j.ijbiomac.2021.03.146.
[150] K. Asadisarvestani, M. Navaee, Demographic and socio-cultural determinants of intended and unintended pregnancies among women under cancer treatment in sistan and Baluchestan province, Iran, Shiraz E-Medical J. 22 (2021).
[151] X. Dong, W. Yin, X. Zhang, S. Zhu, X. He, J. Yu, J. Xie, Z. Guo, L. Yan, X. Liu, Q. Wang, Z. Gu, Y. Zhao, Intelligent MoS2 nanotheranostic for targeted and enzyme-/pH-/NIR-responsive drug delivery to overcome cancer chemotherapy resistance guided by PET imaging, ACS Appl. Mater. Interfaces 10 (2018) 4271–4284, https://doi.org/10.1021/ACSAMI.7B17506/SUPPL_FILE/AM7B17506_SI_001.PDF.
[152] J. Liu, J. Zheng, H. Nie, D. Zhang, D. Cao, Z. Xing, B. Li, L. Jia, Molybdenum disulfide-based hyaluronic acid-guided multifunctional theranostic nanoplatform for magnetic resonance imaging and synergetic chemo-photothermal therapy, J. Colloid Interface Sci. 548 (2019) 131–144, https://doi.org/10.1016/J.JCIS.2019.04.022.
[153] M.J. Khodabakhshi, H.A. Panahi, E. Konoz, A. Feizbakhsh, S. Kimiagar, Synthesis of pH and thermo-sensitive dendrimers based on MoS2 and magnetic nanoparticles for cisplatin drug delivery system by the near-infrared laser, Polym. Adv. Technol. 32 (2021) 1626–1635.
[154] K. Wang, C. Li, Y. Li, J. Wang, A. Ma, The application of hierarchy MoS2 particles for NIR induced drug delivery towards liver cancer treatment, Mater. Res. Express 7 (2020), 105014.
[155] K. Zhang, Y. Zhao, L. Wang, L. Zhao, X. Liu, S. He, NIR-responsive transdermal delivery of atenolol based on polyacrylamide-modified MoS2 nanoparticles, Inorg. Chem. Commun. 122 (2020), 108277.
[156] K. Zhang, Y. Zhuang, J. Li, X. Liu, S. He, Poly (Acrylic acid)-modified MoS2 nanoparticle-based transdermal delivery of atenolol, Int. J. Nanomed. 15 (2020) 5517.
[157] L. Ding, Y. Chang, P. Yang, W. Gao, M. Sun, Y. Bie, L. Yang, X. Ma, Y. Guo, Facile synthesis of biocompatible L-cysteine-modified MoS2 nanospheres with high photothermal conversion efficiency for photothermal therapy of tumor, Mater. Sci. Eng. C 117 (2020), 111371.
[158] S. Cai, J. Yan, H. Xiong, Q. Wu, H. Xing, Y. Liu, S. Liu, Z. Liu, Aptamer-functionalized molybdenum disulfide nanosheets for tumor cell targeting and lysosomal acidic environment/NIR laser responsive drug delivery to realize synergetic chemo-photothermal therapeutic effects, Int. J. Pharm. 590 (2020), 119948.
[159] J. Wang, Z. Li, Y. Yin, H. Liu, G. Tang, Y. Ma, X. Feng, H. Mei, J. Bi, K. Wang, Mesoporous silica nanoparticles combined with MoS2 and FITC for fluorescence imaging and photothermal therapy of cancer cells, J. Mater. Sci. 55 (2020) 15263–15274.
[160] L. Zhou, J. Zhao, Y. Chen, Y. Zheng, J. Li, J. Zhao, J. Zhang, Y. Liu, X. Liu, S. Wang, MoS2-ALG-Fe/GOx hydrogel with Fenton catalytic activity for combined

cancer photothermal, starvation, and chemodynamic therapy, Colloids Surf. B Biointerfaces 195 (2020), 111243.
[161] S. Zhang, L. Jin, J. Liu, Y. Liu, T. Zhang, Y. Zhao, N. Yin, R. Niu, X. Li, D. Xue, Boosting chemodynamic therapy by the synergistic effect of Co-catalyze and photothermal effect triggered by the second near-infrared light, Nano-Micro Lett. 12 (2020) 1–13.
[162] Y. Huang, Q. Gao, X. Li, Y. Gao, H. Han, Q. Jin, K. Yao, J. Ji, Ofloxacin loaded MoS2 nanoflakes for synergistic mild-temperature photothermal/antibiotic therapy with reduced drug resistance of bacteria, Nano Res. 13 (2020) 2340–2350.
[163] C. Wang, J. Li, X. Liu, Z. Cui, D.-F. Chen, Z. Li, Y. Liang, S. Zhu, S. Wu, The rapid photoresponsive bacteria-killing of Cu-doped MoS 2, Biomater. Sci. 8 (2020) 4216–4224.
[164] X. Zhang, Z. Zhao, P. Yang, W. Liu, J. Fan, B. Zhang, S. Yin, MoS2@ C nanosphere as near infrared/pH dual response platform for chemical photothermal combination treatment, Colloids Surf. B Biointerfaces 192 (2020), 111054.
[165] R. Jin, J. Yang, P. Ding, C. Li, B. Zhang, W. Chen, Y.-D. Zhao, Y. Cao, B. Liu, Antitumor immunity triggered by photothermal therapy and photodynamic therapy of a 2D MoS2 nanosheet-incorporated injectable polypeptide-engineered hydrogel combinated with chemotherapy for 4T1 breast tumor therapy, Nanotechnology 31 (2020), 205102.
[166] S. Rajasekar, E.M. Martin, S. Kuppusamy, C. Vetrivel, Chitosan coated molybdenum sulphide nanosheet incorporated with tantalum oxide nanomaterials for improving cancer photothermal therapy, Arab. J. Chem. 13 (2020) 4741–4750.
[167] J. Liu, J. Zheng, H. Nie, H. Chen, B. Li, L. Jia, Co-delivery of erlotinib and doxorubicin by MoS2 nanosheets for synergetic photothermal chemotherapy of cancer, Chem. Eng. J. 381 (2020), 122541.
[168] Y. Yang, J. Wu, D.H. Bremner, S. Niu, Y. Li, X. Zhang, X. Xie, L.-M. Zhu, A multifunctional nanoplatform based on MoS2-nanosheets for targeted drug delivery and chemo-photothermal therapy, Colloids Surf. B Biointerfaces 185 (2020), 110585.
[169] S. Yang, D. Li, L. Chen, X. Zhou, L. Fu, Y. You, Z. You, L. Kang, M. Li, C. He, Coupling metal organic frameworks with molybdenum disulfide nanoflakes for targeted cancer theranostics, Biomater. Sci. 9 (2021) 3306–3318.
[170] K. Kasinathan, K. Marimuthu, B. Murugesan, S. Samayanan, S.J. Panchu, H. C. Swart, S.R.I. Savariroyan, Synthesis of biocompatible chitosan functionalized Ag decorated biocomposite for effective antibacterial and anticancer activity, Int. J. Biol. Macromol. 178 (2021) 270–282.
[171] X. Li, H. Xiao, W. Xiu, K. Yang, Y. Zhang, L. Yuwen, D. Yang, L. Weng, L. Wang, Mitochondria-targeting MoS2-based nanoagents for enhanced NIR-II photothermal-chemodynamic synergistic oncotherapy, ACS Appl. Mater. Interfaces 13 (2021) 55928–55938.
[172] J. Zhao, H. Wu, J. Zhao, Y. Yin, Z. Zhang, S. Wang, K. Lin, 2D LDH-MoS 2 clay nanosheets: synthesis, catalase-mimic capacity, and imaging-guided tumor phototherapy, J. Nanobiotechnol. 19 (2021) 1–16.
[173] L. Cai, L. Dong, X. Sha, S. Zhang, S. Liu, X. Song, M. Zhao, Q. Wang, K. Xu, J. Li, Exfoliation and in situ functionalization of MoS2 nanosheets for MRI-guided combined low-temperature photothermal therapy and chemotherapy, Mater. Des. 210 (2021), 110020.
[174] S. Yougbaré, C. Mutalik, P.-F. Chung, D.I. Krisnawati, F. Rinawati, H. Irawan, H. Kristanto, T.-R. Kuo, Gold nanorod-decorated metallic mos2 nanosheets for synergistic photothermal and photodynamic antibacterial therapy, Nanomaterials 11 (2021) 3064.
[175] A. Abareshi, N. Samadi, M. Houshiar, S. Nafisi, H.I. Maibach, Erythromycin dermal delivery by MoS2 nanoflakes, J. Pharm. Investig. 51 (2021) 691–700.
[176] M. Mohammadi Kalakoo, A. Heydarinasab, E. Moniri, H. Ahmad Panahi, R. Khoshneviszadeh, Near-infrared triggered drug delivery of Imatinib Mesylate by molybdenum disulfide nanosheets grafted copolymers as thermosensitive nanocarriers, Polym. Adv. Technol. 32 (2021) 3253–3265.
[177] S. Khaledian, D. Kahrizi, S.T.J. Balaky, E. Arkan, M. Abdoli, F. Martinez, Electrospun nanofiber patch based on gum tragacanth/polyvinyl alcohol/molybdenum disulfide composite for tetracycline delivery and their inhibitory effect on Gram+ and Gram–bacteria, J. Mol. Liq. 334 (2021), 115989.
[178] K. Kasinathan, K. Marimuthu, B. Murugesan, N. Pandiyan, B. Pandi, S. Mahalingam, B. Selvaraj, Cyclodextrin functionalized multi-layered MoS2 nanosheets and its biocidal activity against pathogenic bacteria and MCF-7 breast cancer cells: synthesis, characterization and in-vitro biomedical evaluation, J. Mol. Liq. 323 (2021), 114631.
[179] L. Chen, J. Xu, Y. Wang, R. Huang, Ultra-small MoS2 nanodots-incorporated mesoporous silica nanospheres for pH-sensitive drug delivery and CT imaging, J. Mater. Sci. Technol. 63 (2021) 91–96.
[180] E.R. Soltani, K. Tahvildari, E. Moniri, H.A. Panahi, NIPAM/PEG/MoS2 nanosheets for dual triggered doxorubicin release and combined chemo-photothermal cancer therapy, Curr. Drug Deliv. (2021).
[181] A. Abareshi, R. Bafkari, M. Houshiar, R. Dinarvand, Molybdenum disulfide/carbon nanocomposite with enhanced photothermal effect for doxorubicin delivery, Eur. Phys. J. Plus. 136 (2021) 1–16.
[182] M.J. Khodabakhshi, H. Ahmad Panahi, E. Konoz, A. Feizbakhsh, S. Kimiagar, NIR-triggered drug delivery system based on Fe3O4-MoS2 core-shell grafted poly (N-vinylcaprolactam): isotherm and kinetics studies, Polym. Technol. Mater. 60 (2021) 1247–1260.
[183] F. Wang, F.-Y. Lv, K.-L. Liu, Z.-H. Li, S. Niu, Y.-Y. Zhang, H.-L. Cong, Y.-Q. Shen, B. Yu, Synthesis of MoS2 nanosheets drug delivery system and its drug release behaviors, Ferroelectrics 578 (2021) 31–39.
[184] Y. Tian, W. Yi, L. Bai, X. Cheng, T. Yi, M. Mu, P. Zhang, J. Si, X. Hou, J. Hou, One-step in situ growth of MoS 2@ lentinan as a dual-stimuli-responsive nanocarrier for synergistic chemo-photothermal therapy, New J. Chem. 45 (2021) 17966–17975.
[185] A. Yuan, Y. Zhang, G. Fang, W. Chen, X. Zeng, H. Zhou, H. Cai, X. Zhong, Ultrasmall MoS2 nanodots-wrapped perfluorohexane nanodroplets for dual-modal imaging and enhanced photothermal therapy, Colloids Surf. B Biointerfaces 205 (2021), 111880.
[186] G. Li, F. Meng, T. Lu, L. Wei, X. Pan, Z. Nong, M. Wei, C. Liao, X. Li, Functionalised molybdenum disulfide nanosheets for co-delivery of doxorubicin and siRNA for combined chemo/gene/photothermal therapy on multidrug-resistant cancer, J. Pharm. Pharmacol. 73 (2021) 1128–1135.
[187] Y. Zhang, Z. He, F. Yang, C. Ye, X. Xu, S. Wang, L. Zhang, D. Zou, Novel PVA-based microspheres Co-loaded with photothermal transforming agent and chemotherapeutic for colorectal cancer treatment, Pharmaceutics 13 (2021) 984.
[188] W. Hu, T. Xiao, D. Li, Y. Fan, L. Xing, X. Wang, Y. Li, X. Shi, M. Shen, Intelligent molybdenum disulfide complexes as a platform for cooperative imaging-guided Tri-mode chemo-photothermo-immunotherapy, Adv. Sci. 8 (2021), 2100165.
[189] T. Ma, X. Zhai, Y. Huang, M. Zhang, X. Zhao, Y. Du, C. Yan, A smart nanoplatform with photothermal antibacterial capability and antioxidant activity for chronic wound healing, Adv. Healthc. Mater. 10 (2021), 2100033.
[190] S. Zhou, X. Jiao, Y. Jiang, Y. Zhao, P. Xue, Y. Liu, J. Liu, Engineering Eu3+-incorporated MoS2 nanoflowers toward efficient photothermal/photodynamic combination therapy of breast cancer, Appl. Surf. Sci. 552 (2021), 149498.
[191] G. Pidamaimaiti, X. Huang, K. Pang, Z. Su, F. Wang, A microenvironment-mediated Cu 2 O–MoS 2 nanoplatform with enhanced Fenton-like reaction activity for tumor chemodynamic/photothermal therapy, New J. Chem. 45 (2021) 10296–10302.
[192] L. Yuwen, Q. Qiu, W. Xiu, K. Yang, Y. Li, H. Xiao, W. Yang, D. Yang, L. Wang, Hyaluronidase-responsive phototheranostic nanoagents for fluorescence imaging and photothermal/photodynamic therapy of methicillin-resistant Staphylococcus aureus infections, Biomater. Sci. 9 (2021) 4484–4495.
[193] B. Pang, H. Yang, L. Wang, J. Chen, L. Jin, B. Shen, Aptamer modified MoS2 nanosheets application in targeted photothermal therapy for breast cancer, Colloids Surfaces A Physicochem. Eng. Asp. 608 (2021), 125506.
[194] L. Liu, X. Pan, S. Liu, Y. Hu, D. Ma, Near-infrared light-triggered nitric oxide release combined with low-temperature photothermal therapy for synergetic antibacterial and antifungal, Smart Mater. Med. 2 (2021) 302–313.
[195] S. Li, S. Yang, C. Liu, J. He, T. Li, C. Fu, X. Meng, H. Shao, Enhanced photothermal-photodynamic therapy by indocyanine green and curcumin-loaded layered MoS2 hollow spheres via inhibition of p-glycoprotein, Int. J. Nanomed. 16 (2021) 433.
[196] F. Jiang, B. Ding, S. Liang, Y. Zhao, Z. Cheng, B. Xing, J. Lin, Intelligent MoS2–CuO heterostructures with multiplexed imaging and remarkably enhanced antitumor efficacy via synergetic photothermal therapy/chemodynamic therapy/immunotherapy, Biomaterials 268 (2021), 120545.
[197] W. Zhang, M. Ding, H. Zhang, H. Shang, A. Zhang, Tumor acidity and near-infrared light responsive drug delivery MoS 2 -based nanoparticles for chemo-photothermal therapy, Photodiagnosis Photodyn. Ther. 38 (2022). https://www.clinicalkey.com/#!/content/journal/1-s2.0-S1572100022000059.
[198] J. Li, N. Yang, M. Yang, C. Lu, M. Xie, Development of a magnetic MoS2 system camouflaged by lipid for chemo/phototherapy of cancer, Colloids Surf. B Biointerfaces 213 (2022), 112389.
[199] Y. Li, R. Fu, Z. Duan, C. Zhu, D. Fan, Construction of multifunctional hydrogel based on the tannic acid-metal coating decorated MoS2 dual nanozyme for bacteria-infected wound healing, Bioact. Mater. 9 (2022) 461–474.
[200] S. Guan, X. Liu, Y. Fu, C. Li, J. Wang, Q. Mei, G. Deng, W. Zheng, Z. Wan, J. Lu, A biodegradable "Nano-donut" for magnetic resonance imaging and enhanced chemo/photothermal/chemodynamic therapy through responsive catalysis in tumor microenvironment, J. Colloid Interface Sci. 608 (2022) 344–354.
[201] Z. Zhao, P. Yang, X. Zhang, J. Lin, J. Fan, B. Zhang, Combination of chemotherapy and photothermal methods for in vitro ablation of MCF-7 cancer cells using crinkly core–shell structure MoS2/C@ SiO2 nanospheres, Adv. Powder Technol. 33 (2022), 103388.
[202] M. Dong, X. Sun, T. Bu, H. Zhang, J. Wang, K. He, L. Li, Z. Li, L. Wang, 3D/2D TMSs/TiO2 nanofibers heterojunctions for photodynamic-photothermal and oxidase-like synergistic antibacterial therapy co-driven by VIS and NIR biowindows, Compos. B Eng. 230 (2022), 109498.
[203] H. Li, M. Gong, J. Xiao, L. Hai, Y. Luo, L. He, Z. Wang, L. Deng, D. He, Photothermally activated multifunctional MoS2 bactericidal nanoplatform for combined chemo/photothermal/photodynamic triple-mode therapy of bacterial and biofilm infections, Chem. Eng. J. 429 (2022), 132600.
[204] Y. Li, R. Fu, Z. Duan, C. Zhu, D. Fan, Adaptive hydrogels based on nanozyme with dual-enhanced triple enzyme-like activities for wound disinfection and mimicking antioxidant defense system, Adv. Healthc. Mater. 11 (2022), e2101849.
[205] Y. Cao, K. Wang, P. Zhu, X. Zou, G. Ma, W. Zhang, D. Wang, J. Wan, Y. Ma, X. Sun, A near-infrared triggered upconversion/MoS2 nanoplatform for tumour-targeted chemo-photodynamic combination therapy, Colloids Surf. B Biointerfaces 213 (2022), 112393.
[206] X. Wang, T. Li, H. Ma, D. Zhai, C. Jiang, J. Chang, J. Wang, C. Wu, A 3D-printed scaffold with MoS2 nanosheets for tumor therapy and tissue regeneration, NPG Asia Mater. 2017 94 (2017), https://doi.org/10.1038/am.2017.47, 9, e376–e376.
[207] K. Ma, C. Liao, L. Huang, R. Liang, J. Zhao, L. Zheng, W. Su, Electrospun PCL/MoS2 nanofiber membranes combined with NIR-triggered photothermal therapy to accelerate bone regeneration, Small 17 (2021), 2104747.

[208] H. Nazari, A. Heirani-Tabasi, M.S. Alavijeh, Z.S. Jeshvaghani, E. Esmaeili, S. Hosseinzadeh, F. Mohabatpour, B. Taheri, S.H.A. Tafti, M. Soleimani, Nanofibrous composites reinforced by MoS2 Nanosheets as a conductive scaffold for cardiac tissue engineering, ChemistrySelect 4 (2019) 11557–11563.
[209] S. Wang, J. Qiu, W. Guo, X. Yu, J. Nie, J. Zhang, X. Zhang, Z. Liu, X. Mou, L. Li, A nanostructured molybdenum disulfide film for promoting neural stem cell neuronal differentiation: toward a nerve tissue-engineered 3D scaffold, Adv. Biosyst. 1 (2017), 1600042.
[210] Y. Liu, X. Zhao, C. Zhao, H. Zhang, Y. Zhao, Responsive porous microcarriers with controllable oxygen delivery for wound healing, Small 15 (2019), 1901254.
[211] G.P. Awasthi, V.K. Kaliannagounder, B. Maharjan, J.Y. Lee, C.H. Park, C.S. Kim, Albumin-induced exfoliation of molybdenum disulfide nanosheets incorporated polycaprolactone/zein composite nanofibers for bone tissue regeneration, Mater. Sci. Eng. C 116 (2020), 111162.
[212] H. Wang, X. Zeng, L. Pang, H. Wang, B. Lin, Z. Deng, E.L.X. Qi, N. Miao, D. Wang, P. Huang, Integrative treatment of anti-tumor/bone repair by combination of MoS2 nanosheets with 3D printed bioactive borosilicate glass scaffolds, Chem. Eng. J. 396 (2020), 125081.
[213] H. Nazari, A. Heirani-Tabasi, M. Hajiabbas, M. Khalili, M. Shahsavari Alavijeh, S. Hatamie, A. Mahdavi Gorabi, E. Esmaeili, S.H. Ahmadi Tafti, Incorporation of two-dimensional nanomaterials into silk fibroin nanofibers for cardiac tissue engineering, Polym, Adv. Met. Technol. 31 (2020) 248–259.
[214] F. Qi, X. Gao, S. Peng, W. Yang, G. Qian, S. Yang, C. Shuai, Polyaniline protrusions on MoS2 nanosheets for PVDF scaffolds with improved electrical stimulation, ACS Appl. Nano Mater. 4 (2021) 13955–13966.
[215] J. Luo, Q. Zhou, X. Hu, X. Hou, D. Li, S. Guo, S. Sun, Magnetic field-guided MoS2/WS2 heterolayered nanofilm Regulates cell behavior and gene expression, ACS Appl. Nano Mater. 4 (2021) 10828–10835.
[216] Z. Zohreband, M. Adeli, A. Zebardasti, Self-healable and flexible supramolecular gelatin/MoS2 hydrogels with molecular recognition properties, Int. J. Biol. Macromol. 182 (2021) 2048–2055.
[217] H. Nazari, A. Heirani-Tabasi, E. Esmaeili, A.-M. Kajbafzadeh, Z. Hassannejad, S. Boroomand, M.H. Shahsavari Alavijeh, M.A. Mishan, S.H. Ahmadi Tafti, M. E. Warkiani, Decellularized human amniotic membrane reinforced by MoS2-Polycaprolactone nanofibers, a novel conductive scaffold for cardiac tissue engineering, J. Biomater. Appl. (2022), 08853282211063289.
[218] J. Zhang, B. Zhang, Z. Zheng, Q. Cai, J. Wang, Q. Shu, L. Wang, Tissue-Engineered bone functionalized with MoS2 nanosheets for enhanced repair of critical-size bone defect in rats, Adv. Funct. Mater. 32 (2022), 2109882.
[219] N. Mphuthi, L. Sikhwivhilu, S.S. Ray, Functionalization of 2D MoS2 nanosheets with various metal and metal oxide nanostructures: their properties and application in electrochemical sensors, Biosensors 12 (2022) 386, https://doi.org/10.3390/bios12060386.
[220] T. Liu, Z. Liu, 2D MoS2 nanostructures for biomedical applications, Adv. Healthc. Mater. 7 (2018), 1701158, https://doi.org/10.1002/ADHM.201701158.
[221] J. Kabel, S. Sharma, A. Acharya, D. Zhang, Y.K. Yap, Molybdenum Disulfide Quantum Dots: Properties, Synthesis, and Applications, C, vol. 7, 2021, p. 45, https://doi.org/10.3390/c7020045.
[222] M. Pumera, A.H. Loo, Layered transition-metal dichalcogenides (MoS2 and WS2) for sensing and biosensing, TrAC, Trends Anal. Chem. 61 (2014) 49–53, https://doi.org/10.1016/j.trac.2014.05.009.
[223] K. Kalantar-Zadeh, J.Z. Ou, Biosensors based on two-dimensional MoS2, ACS Sens. 1 (2016) 5–16, https://doi.org/10.1021/ACSSENSORS.5B00142/ASSET/IMAGES/MEDIUM/SE-2015-00142C_0007 (GIF).
[224] V. Yadav, S. Roy, P. Singh, Z. Khan, A. Jaiswal, 2D MoS2-based nanomaterials for therapeutic, bioimaging, and biosensing applications, Small 15 (2019), 1803706, https://doi.org/10.1002/SMLL.201803706.
[225] Z. Cui, D. Li, W. Yang, K. Fan, H. Liu, F. Wen, L. Li, L. Dong, G. Wang, W. Wu, An electrochemical biosensor based on few-layer MoS2 nanosheets for highly sensitive detection of tumor marker ctDNA, Anal. Methods 14 (2022), https://doi.org/10.1039/D2AY00467D, 1956–1962.
[226] Y.S. Zhang, J. Yao, Imaging Biomaterial–tissue interactions, Trends Biotechnol. 36 (2018) 403–414, https://doi.org/10.1016/j.tibtech.2017.09.004.
[227] N.S. Arul, V.D. Nithya, Molybdenum disulfide quantum dots: synthesis and applications, RSC Adv. 6 (2016) 65670–65682, https://doi.org/10.1039/C6RA09060E.
[228] S. Roy, Y. Bobde, B. Ghosh, C. Chakraborty, Targeted bioimaging of cancer cells using free folic acid-sensitive molybdenum disulfide quantum dots through fluorescence “turn-off, ACS Appl. Bio Mater. 4 (2021) 2839–2849, https://doi.org/10.1021/ACSABM.1C00090/ASSET/IMAGES/MEDIUM/MT1C00090_0012 (GIF).